THE UNIVERSITY OF OKLAHOMA

GRADUATE COLLEGE

APPLICATION OF THE DIFFUSION WIND ATMOSPHERIC DISPERSION MODEL TO THE TULSA URBAN AREA

A DISSERTATION

SUBMITTED TO THE GRADUATE FACULTY

in partial fulfillment of the requirements for the

degree of

DOCTOR OF PHILOSOPHY

By

Jack D. Shannon

Norman, Oklahoma

1975

APPLICATION OF THE DIFFUSION WIND ATMOSPHERIC DISPERSION MODEL TO THE TULSA URBAN AREA

A DISSERTATION

APPROVED FOR THE DEPARTMENT OF METEOROLOGY

By

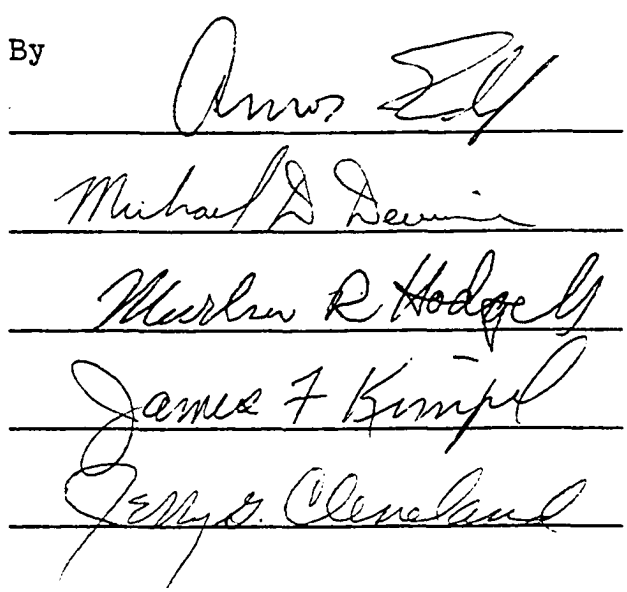

ACKNOWLEDGMENTS

I wish to express my appreciation to Dr. Amos Eddy for his investigative insight, his invaluable contacts, and his financial support during most of my drawn-out graduate study.

Thanks are due to Dr. Merlin Hodgell, Dr. Mike Devine, Dr. Jeff Kimpel, and Dr. Jerry Cleveland for their helpful advice and patience. The data provided by Dr. Cleveland and the Tulsa City/County Health Board were essential.

Mr. Patrick Brady and Mr. Tom Wright gave me much assistance with graphics wrenched from obstinate computers.

Most of all, I am deeply grateful to Mrs. Margaret Eddy for her counsel and friendship when I considered saying something obscene and departing.

TABLE OF CONTENTS

LIST OF TABLES

LIST OF ILLUSTRATIONS

FIGURE Page

APPLICATION OF THE DIFFUSION WIND ATMOSPHERIC DISPERSION MODEL TO THE TULSA URBAN AREA

CHAPTER I

INTRODUCTION

Public officials and the general populace are becoming more aware of the health risks associated with the various air pollutants endemic to modern industrial society. Many laws and regulations have been written during recent years. Some have even been enforced. This aspect of the environment may be regulated even more in the future, with air quality being checked more frequently for more pollutants.

Tools are required in order to accomplish the clean air goals which are being defined over a period of time by general consensus of the nation. Some of these tools are technological, such as more efficient pollution control equipment and new instrumentation for measurement of pollution concentrations and meteorological parameters. Some tools are conceptual, involving understanding and simulation of the processes involved in dispersion of air pollution and the prediction of resulting concentrations. Some tools are

educational, such as methods which demonstrate to non-scientific viewers and readers the significant features of air pollution problems.

There is no single dispersion model which fulfills all of the varied needs of scientific researchers, decision makers, and the interested public. There are definite needs and opportunities for a variety of dispersion models. Most contemporary models are devised to predict concentrations over a short time period, such as 30 minutes, in which meteorological conditions and emission rates are constant, or to predict annual concentrations through climatological weighting of short-term periods. The diffusion wind atmospheric dispersion model fills a niche for dispersion models which predict patterns of concentration for periods from several hours up to a week or ten days. Such periods are long enough for conditions to vary, but short enough to create problems in weighting of short-term predictions.

The diffusion wind model has been devised to treat many problems of dispersion in a manner understandable to non-technical users. The model allows wind, stability, and emission variations in space and time, and contains options to allow examination of specific modeling questions. The time and space variation capability of the model make it very amenable to production of short films for visual presentation of results.

The basic diffusing method of the diffusion wind

model was developed as part of my master's degree thesis (Shannon, 1972). Input data and results of the model shown in the thesis were strictly simulations. At that time the diffusion technique was basically an engineering or practical approach to the prediction of dispersion; an explanation of the relationship of the diffusion wind model to other dispersion models was not thoroughly developed.

In this research, the diffusion wind model is applied to the Tulsa, Oklahoma urban area, with real emission and meteorological data. Tulsa was selected because it is a city of medium size with only a few significant industrial sources, built upon relatively flat, homogeneous terrain, and isolated from heavy industrial regions. In addition, a good working relationship with personnel of the Tulsa City/County Health Board helped immensely in data acquisition. Results are compared to observed measurements of air quality, where available, and a theoretical basis of the model is developed.

A brief description of state-of-the-art dispersion models is given in Chapter II. The basic diffusion method of the diffusion wind model is then explained, along with key algorithms of the model. Input data requirements and output of results are explained.

Chapter III shows sensitivity tests for the diffusion wind model under different data and modeling assumptions. In general, one parameter or assumption is varied at a time and side by side spatial or temporal comparisons of predictions

are shown.

Chapter IV compares predicted results from the diffusion wind model to observed pollution concentrations. Results are mixed, with some predictions quite close to measured values while others exhibit wide differences. Possible sources of error are considered.

Techniques and potential for future applications and extensions of the diffusion wind model are analyzed in Chapter V. A method for rigorous calibration of the model for a particular city or urban region is discussed.

A summary of the research accomplished and conclusions drawn from results are given in Chapter VI. Mathematics of the relationship of the diffusion wind model to a Gaussian model, method of calculation of traffic emissions, and explanation of a climate generator for use in model simulations are shown in Appendices A-C, respectively.

CHAPTER II

THE DIFFUSION WIND ATMOSPHERIC DISPERSION MODEL

The diffusion wind atmospheric model was developed in order to meet the need for dispersion models which treat situations of a few hours to a week in duration, in which the temporal sequence of spatially varying meteorological parameters and the temporal patterns of emission are important. For short-term (≈30 minute) prediction, current models do not treat temporal variations, while for long-term or annual prediction the temporal sequence of spatial variation is not important. Contemporary dispersion models are briefly examined in section A of this Chapter, with a look at the major features of Gaussian and box models.

In section B the diffusion wind model is shown to be most nearly a box model. A general description of the diffusion wind model is given, including the physical representation of the atmosphere and an explanation of the basic diffusion technique, the diffusion wind. A comparison is made to the diffusion method of the Particle-in-Cell technique (Sklarew, Fabrick, and Prager, 1971).

The form and extent of the input data requirements for the diffusion wind model are shown in section C, with particular emphasis given to meteorological data. Section D describes the output of prediction results of the model.

The key algorithms of the diffusion wind model are described in section E, including translation of box "clouds" of pollution, allocation of those clouds to the grid system, initial layer assignment of plume height (partly Gaussian), and time step determination. A technique for avoidance of a computational secondary diffusion mechanism is also given.

A. Contemporary Dispersion Models

State-of-the-art dispersion models have been classified by Singer and Freudenthal (1972) into two basic types. The most widely applied models are versions of a Gaussian plume, as described by Turner (1969). The key feature of the Gaussian model is the assumption that the pollutants in the plume are distributed in a Gaussian fashion about the plume centerline, both transversely and vertically. The parameters which describe the Gaussian distribution vary with distance downstream from the source and with stability. Application of the model is fairly simple, due to the fact that concentrations are predicted from an equation, and thus computation time is very short (for a single point prediction). The basic model contains

a number of restrictive assumptions, such as a spatially and temporally constant wind, stability, and emission rate. Application of the Gaussian plume distribution theory to specific modeling questions has led to a number of modified Gaussian models. Among these are the Climatological Dispersion Model or CDM (Busse and Zimmerman, 1973), which uses a narrow plume (22.5°) hypothesis and is widely applied to predictions of annual concentrations, and the Tennessee Valley Authority (TVA) models (Montgomery, et al., 1973) for prediction of short-term maximum concentrations under specific dispersion conditions of fumigation, plume trapping, and coning. The TVA models were developed from a combination of theory and observation.

The other basic dispersion model type is the box model, which is in large part an outgrowth of numerical weather prediction techniques. Box models represent the atmosphere with a grid, solve the turbulent diffusion equation or some similar equation, and are often used to model temporal variations of emissions and meteorology; box models normally require iterative steps and more complex calculations than Gaussian models. One of the most advanced box models is the Particle-in-Cell method of Sklarew, Fabrick, and Prager (1971). The model is based upon the use of Lagrangian mass points and disperses by solution of the turbulent diffusion equation.

B. General Model Description

The diffusion wind atmospheric dispersion model could be classified as a box model, although not strictly according to the definition of Singer and Freudenthal, since the model is not based upon the finite difference solution of an equation. The diffusion wind model depicts the atmosphere in multiblock layers. Pollution concentrations are represented by the mass of pollutant inside each block, and can easily be converted to micrograms per cubic meter values, the form most common in air quality regulations.

The number of blocks along each of the horizontal axes is an input to the model, as is the number of layers. The optimal choice for the extent of the modeled atmosphere should reflect the particular situation to which the model is being applied, as well as data availability and computer capability. Normally the two horizontal dimensions of blocks are equal, but the number of blocks along each axis may be varied because of asymmetry in source locations or wind direction frequencies. Depth of different layers can be varied, with shallow layers normally at the bottom of the modeled atmosphere. Grid block dimensions create a limit to spatial resolution of the air pollution field, and it is important to have the best resolution near the surface where people and air quality monitors are located.

The pollutant emission of a source enters the calculations of the model as a mass of pollutant per time step emitted into the proper block or blocks. The temporal resolution of an emission rate is thus bounded by the duration of a time increment. The spatial resolution of source emission is limited by the block dimensions, as the diffusion wind model does not consider the relative position of a source within the block, once the emission is allotted or partially allotted to that block. Multiple sources inside a block are treated as a single source with emission rate equal to the combined multiple sources. Since the block is the limit of spatial resolution, all sources are treated as area sources at a specific elevation interval; thus they might be termed volume sources. Line sources can be approximated by a linear combination of blocks, while point sources can be more finely modeled only by decreasing block dimensions.

The theory and algorithms of the diffusion wind model can be more easily explained if each block is visualized at the beginning of a time step as a separate cloud of pollution, with the concentration constant inside the block. The total pollution field is thus constructed from the spatial combination of the block clouds.

The most interesting feature of the diffusion wind model, and the basis for the name of the model, is the technique used to accomplish diffusion. Each block cloud is expanded in turn by "diffusion wind components", which translate the walls defining the cloud outward, thereby increasing

cloud volume and decreasing the effective concentration. The diffusion wind components (u_D, v_D, w_D) correspond in orientation to the regular wind components (u, v, w); however, the diffusion wind components have magnitude only, as the sign or direction is determined by the diffusion algorithm. A cloud wall originally common to two different blocks would be translated outward according to whichever block was being diffused, and thus the direction of the diffusion wind component at that wall would not be uniquely determined. If the diffusion wind components are relatively large, the diffusion process is rapid. If the diffusion wind components are relatively small, the diffusion process is slow. The key to calibration of the model is determination of the proper magnitude for the diffusion wind components. A formula has been developed which relates the diffusion wind components to block dimensions, time increment, and stability. The derivation of the formula is shown in Appendix A.

After each of the pollution clouds has been advected by the regular wind and diffused (expanded) by the diffusion wind, the results must be allocated back to the model grid. The allocation technique is shown in section E.

There is a similarity in the dispersion algorithm of the diffusion wind model and the dispersion method of the Particle-in-Cell (PICK) technique (Sklarew, et al., 1971). The PICK technique solves the turbulent diffusion equation,

$$\frac{\partial \chi}{\partial t} = - \bar{u} \frac{\partial \chi}{\partial x} - \bar{v} \frac{\partial \chi}{\partial y} - \bar{w} \frac{\partial \chi}{\partial z} + \frac{\partial}{\partial x}\left[K_x \frac{\partial \chi}{\partial x}\right] + \frac{\partial}{\partial y}\left[K_y \frac{\partial \chi}{\partial y}\right] + \frac{\partial}{\partial z}\left[K_z \frac{\partial \chi}{\partial z}\right] \quad (1)$$

where χ is the pollutant concentration; x, y, and z are the Cartesian coordinates; t is time; $\bar{u}$, $\bar{v}$, and $\bar{w}$ are wind components; and K_x, K_y, and K_z are eddy diffusivities. By defining turbulent flux velocity components

$$u_f = \frac{-K_x}{\chi} \frac{\partial \chi}{\partial x} , \quad v_f = \frac{-K_y}{\chi} \frac{\partial \chi}{\partial y} , \quad w_f = \frac{-K_z}{\chi} \frac{\partial \chi}{\partial z} , \quad (2a\text{-}c)$$

further defining total equivalent transport velocity components

$$u_t = u_f + \bar{u}, \quad v_t = v_f + \bar{v}, \quad w_t = w_f + \bar{w}, \quad (3a\text{-}c)$$

and assuming the equation of continuity for an incompressible fluid

$$\frac{\partial \bar{u}}{\partial x} + \frac{\partial \bar{v}}{\partial y} + \frac{\partial \bar{w}}{\partial z} = 0 , \quad (4)$$

rearrangement of terms reduces the turbulent diffusion equation to

$$\frac{\partial \chi}{\partial t} + \frac{\partial u_t \chi}{\partial x} + \frac{\partial v_t \chi}{\partial y} + \frac{\partial w_t \chi}{\partial z} = 0. \quad (5)$$

The mass particles move according to the total equivalent transport velocity components (u_t, v_t, w_t), which are composed of the mean velocity field ($\bar{u}$, $\bar{v}$, $\bar{w}$) and the turbulent flux velocity components (u_f, v_f, w_f). The magnitude and direction of the turbulent flux velocity components

are computed from the eddy diffusivities and the concentration field.

The major difference between the Sklarew turbulent flux velocity components and the diffusion wind components is that the Sklarew components are a function of the concentration field as well as being a function of the eddy diffusivities, and the Sklarew components actually form a vector field. The diffusion wind components are a scalar function of stability, time step, and block dimensions, and are not related to the concentration field. A side benefit of that independence is that the diffusion wind model is not subject to the computational stability considerations of most box models.

C. Data Requirements

The input data required for the diffusion wind model are of three general categories: parameters describing the particular situation being modeled, meteorological data, and emission data. When the diffusion wind model is applied to an operational or historical situation, calibration is needed. This requires a fourth type of data, the measurement of air pollution concentrations over a specified averaging period at various locations.

Situation parameters include the number of layers to be modeled, the number of blocks along each horizontal axis, block dimensions, the pollutant being dispersed, meteorological treatment, whether the pollutant is deposited or reflected at the surface, duration and time of onset of modeled dispersion,

chemical decomposition rate, which plume rise formula, which type of sources, fall speed, and nonmethane percentage of total hydrocarbons (for hydrocarbon dispersion).

The meteorological data depend upon the meteorological treatment option. Observed twenty-four hour mean values may be input (speed and direction of the vector resultant of the twenty-four hourly observations, arithmetic average wind speed, and percentage of possible sunshine occurring), a series of three hourly data may be input (observed wind speed, wind direction, and cloud coverage), a fixed meteorological situation may be input, or the climate generator may be used to generate daily mean values. Wind speeds are expressed in meters per second.

The final form of meteorological data used in the diffusion wind model, as well as in most other dispersion models, are the wind field specified in space and time, and an indicator or indicators of the stability or mixing field specified in space and time. Wind speed and wind direction vary temporally and vertically in the diffusion wind model. The horizontal variations across Tulsa of wind speed and direction, though occurring in reality, are not known well enough to specify. The difficulty is practical and not theoretical. The average hourly variations of wind speed and direction, relative to the twenty-four hour resultant surface layer wind, are input for each layer. The variations were abstracted from Crawford and Hudson (1970), who analysed

data collected on an instrumented television tower in Oklahoma City. Oklahoma City data were used because vertical variations of wind and stability from Tulsa observations are not available in a useful form.

Figure 1 shows the daily pattern of average wind speed for each level in the Crawford and Hudson study, while Figure 2 shows the daily pattern of average wind direction for each level. Average diurnal direction variation of the lower three levels was like that of the surface. The heights of levels 1-6 were 45, 90, 177, 266, 355, and 445 meters, respectively. Since midpoints of the layers of the diffusion wind model do not correspond to specific tower levels, interpolation was necessary when temporal patterns of variation relative to the daily surface means were abstracted.

When three-hourly surface observations are input, hourly surface values are obtained through interpolation. The arrays containing the average daily variation patterns of wind speed and direction are then expressed relative to the hourly surface wind rather than to the daily resultant wind. If a fixed meteorological situation is input, the average wind variation arrays are not used.

Unless the Pasquill-Gifford stability class is specified, the hourly cloud coverage and layer wind speeds are used to compute a stability class for each layer in a manner similar to the classifications used by Turner (1969). Turner's classifications, which are shown in Table 1, are used for the surface layer of the diffusion wind model, while

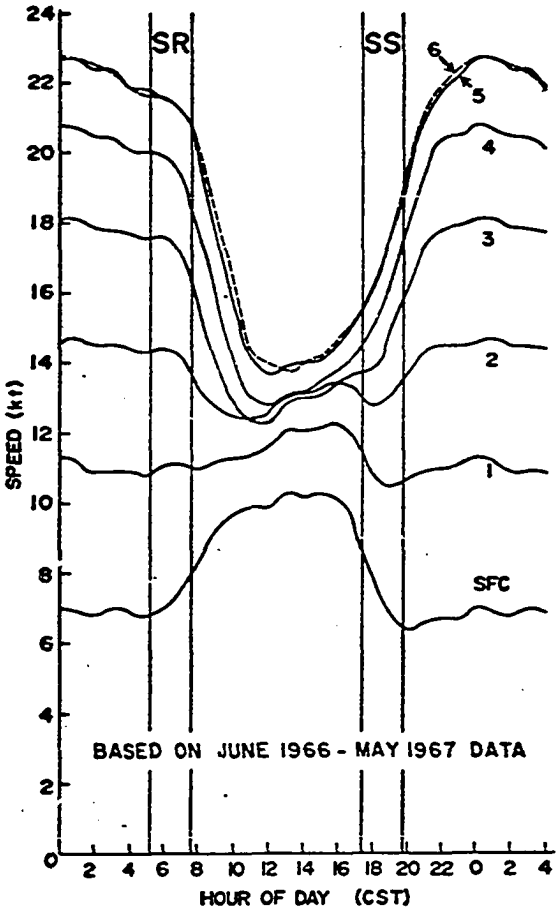

Figure 1: Diurnal variations of mean wind speeds on an annual basis.

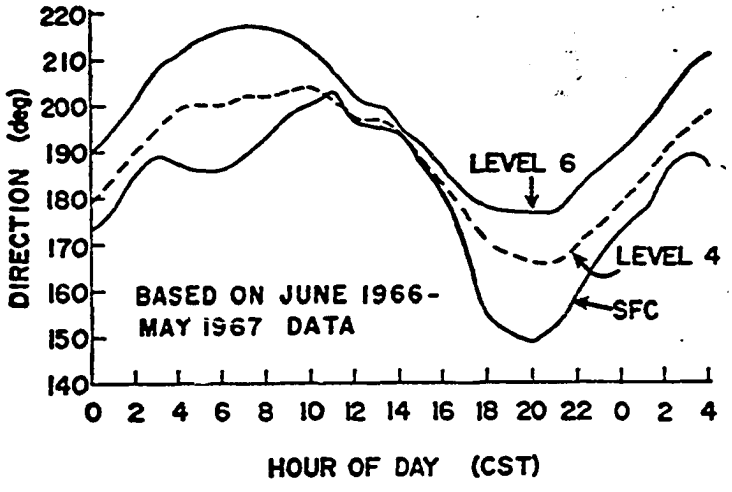

Figure 2: Diurnal variations of the resultant direction on an annual basis for the surface level and levels 4 and 6.

the critical speed categories are arbitrarily increased 0.5 meters per second for each successive class upward. Stability thus varies temporally and vertically.

TABLE 1.--Key to Stability Categories.

Surface Wind Speed (at 10 m), m sec^{-1}	Day			Night	
	Incoming Solar Radiation			Thinly Overcast or ≥4/8 Low Cloud	≤3/8 Cloud
	Strong	Moderate	Slight		
< 2	A	A-B	B		
2-3	A-B	B	C	E	F
3-5	B	B-C	C	D	E
5-6	C	C-D	D	D	D
> 6	C	D	D	D	D

The neutral class, D, should be assumed for overcast conditions during day or night.

(Class A is the most unstable; class F is the most stable. Night refers to the period from one hour before sunset to one hour after sunrise. Strong incoming solar radiation corresponds to a solar altitude greater than 60 degrees with clear skies; slight insolation corresonds to a solar altitude of 15-35 degrees with clear skies.)

Upward propagation with time of daytime instability and nighttime stability, according to results shown by Goff and Hudson (1972) is accomplished by an algorithm which defines effective times of beginning and ending of solar heating which are one hour later for layers 3 and 4 than for layers 1 and 2, and an additional hour later for layers 5 and 6.

Emission data which are input include point source stack parameters and emission rates for each pollutant (particulates, sulfur dioxide (SO_2), nitrogen dioxide (NO_2), hydrocarbons (HC), and carbon monoxide (CO)), traffic emissions by pollutant and square mile (method of computation discussed in Appendix B), and service station hydrocarbon emissions. The daily and weekly variations in traffic and service station emissions, abstracted in part from Roth, et al. (1974), must also be input, in order that the average emission rate may be adjusted by hour and day of the week. Figure 3 illustrates the location of industrial point sources, with a background of Tulsa features for orientation.

Pollution measurements available for comparison to model predictions consist of twenty-four hour average surface concentrations, except for carbon monoxide concentrations which are measured hourly.

D. Output of the Model

The output of the diffusion wind model can easily be varied, depending upon what information is desired. Currently the surface layer concentrations, converted to micrograms per cubic meter (milligrams per cubic meter in the case of carbon monoxide), are printed or punched for each hour and for the daily average. For purposes of later three-dimensional plotting or objective analysis, the concentration for each layer could be stored on tape. Tape storage of fields is also necessary when movies are produced, because

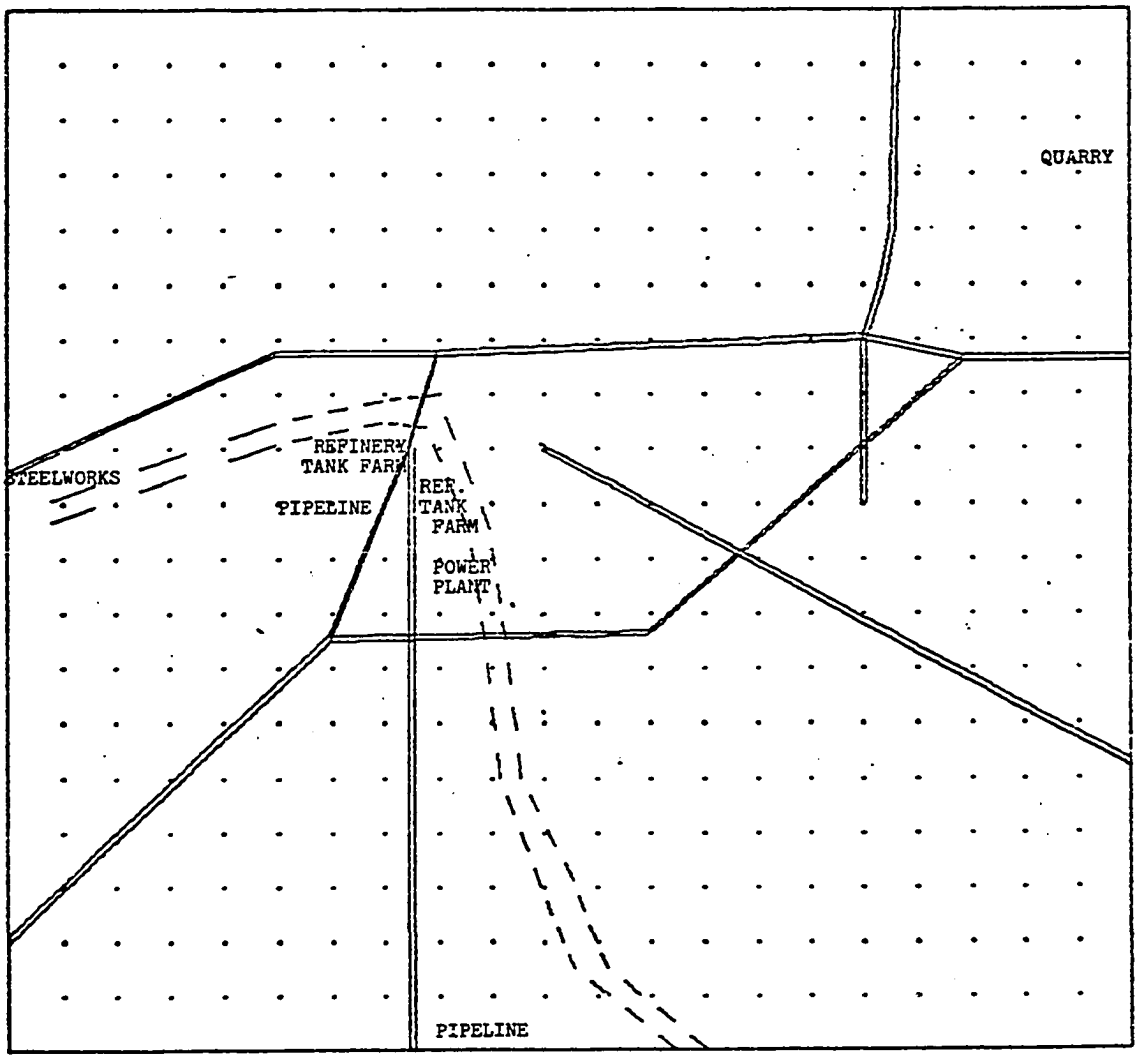

Figure 3: Location of major industrial point sources in the Tulsa urban area. Dashed lines depict Arkansas River; solid lines depict major freeways. Grid points are one mile apart.

of the large number of different concentration fields in the time sequence.

Most of the results shown in Chapters III and IV are presented as contoured fields of pollutant surface concentration over a background of the major Tulsa freeways and the Arkansas River. The same background was used in the movies from computer graphic presentation of model results. This was found to be a useful orientation aid for viewers.

E. Key Algorithms of the Diffusion Wind Model

1. Translation

Since the version of the diffusion wind model applied to the Tulsa urban area does not treat horizontal variations of wind and stability, the relative translation by the processes of advection and diffusion of the pollution clouds defined by the grid block walls is identical for each block within a particular layer. Advection is due to the regular wind components, while diffusion is due to the diffusion wind components. Each time the meteorology changes, translated wall positions relative to the initial positions must be computed only once for each layer. Translation positions for each block cloud in the layer are obtained by adding the grid positions of the blocks to the relative translation.

2. Allocation

After a translation step has occurred, the cloud of pollution which originally coincided with a grid block has a

different position relative to the underlying grid system. The pollution mass inside the cloud is allocated to the underlying grid blocks according to the fraction of the volume of the cloud contained within each block. When all pollution clouds have been allocated and new emissions added to the proper blocks, the new pollution concentration field has been calculated. A two-dimensional example of the allocation routine is shown in Figure 4.

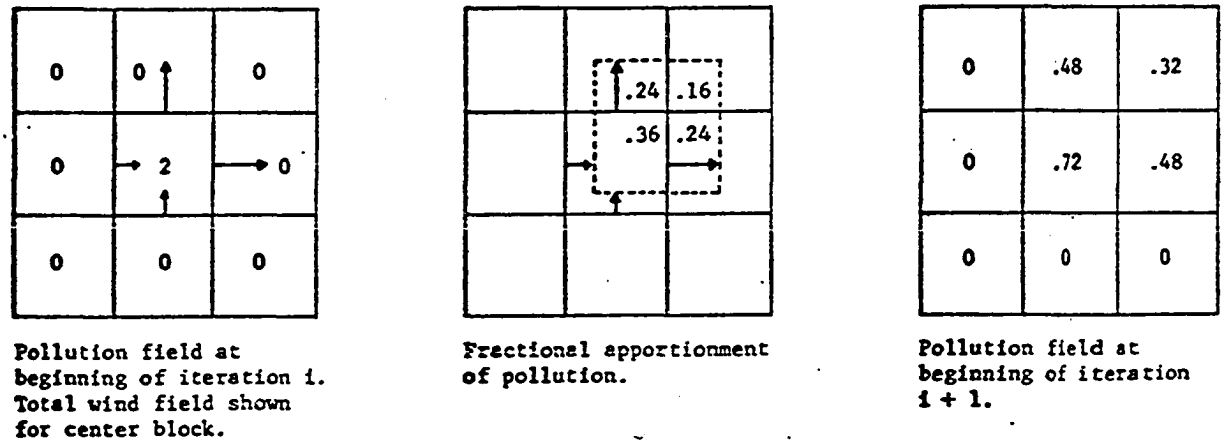

Figure 4: Two-dimensional example of block "cloud" allocation technique.

The key to the allocation algorithm is determination of which of twenty-seven possible configurations, relative to the grid system, is assumed by a translated cloud. There are three possible configurations along each axis: opposite walls within the same grid interval, opposite walls in adjacent grid intervals, or opposite walls with a grid interval intervening. (A limitation on the time step prevents further separation.) The particular grid intervals containing the

translated walls are determined along with the fraction of wall separation distance contained within each interval. The fractions are then used to compute volume fractions used for pollutant mass allocation.

3. Initial Layer Assignment

Early simulations performed with the diffusion wind model assigned the entire time step emission of a point source to the layer into which the plume was calculated to rise. This algorithm, combined with the assumption that any emission into a block is evenly distributed throughout that block, caused the model to be discretely rather than quasi-continuously sensitive to changes in plume rise formula or meteorological parameters. A change of formula caused no alteration in resulting surface concentrations until the plume was computed to lie within a different layer, at which time calculated concentrations could change abruptly. Change in wind speed or stability always led to different predicted concentrations, but that was solely due to changes in advection and diffusion until the change was enough to place the plume in a different layer.

An algorithm was developed to create an initial vertical plume spread. The plume is given a Gaussian distribution in the vertical, centered about the predicted plume height and with the vertical spread a function of stability. The initial vertical spread of the plume varies from 10 meters for the very stable case to 35 meters for the very unstable case. The range of the initial plume spread is arbitrary, but

it is similar to initial spread in the CDM model. The emitted mass is allotted to the different layers according to the fraction of the Gaussian distribution contained within those layers. All of the plume may still be contained within one layer, particularly if the plume rises into the thicker upper layers, but results are considerably less sensitive to small changes in calculated plume height.

The model does not allow industrial point sources to have a plume height which is less than one half of the initial plume vertical spread for the stability class occurring. If there were no plume height minimum, low-level sources lacking a stack parameter value would always be placed in the lowest layer, regardless of its depth. This would lead to predictions being dependent upon the depth of the lower layer (and the implied volume). The value used for the minimum plume height was selected because it avoids initial deposition or reflection of the plume.

Emissions due to traffic and service stations are evenly distributed through the bottom three layers (35 meters). While the actual emissions are in the bottom layer, by the time emissions are blown into the next square mile the pollutants are distributed through a deeper layer. An initial depth of 35 meters was selected because it gave the best results.

4. Time Step Determination

When allocation and emission algorithms take place,

the model assumes that any pollutant mass inside a grid block is evenly distributed throughout that block. Over a sequence of time steps, the assumption acts as a secondary diffusion mechanism, with the relative importance of the secondary mechanism increasing when advection of cloud walls is a small fraction of a grid interval.

In the case of pure diffusion, this secondary diffusion mechanism would cause a block cloud or a plume to be diffused outward along each axis one grid length per time step, regardless of the grid size. In order to minimize secondary diffusion, the time step should be such that a cloud wall is advected one grid interval. In such a case, if the diffusion winds were set equal to zero (no modeled diffusion), only pure advection would be occurring. Since wind speed varies by layer and normally by component in the layer, a single time increment will not satisfy the desired advection distance for all layers. The time increment is selected by dividing the maximum wind component of the fourth layer into the horizontal grid increment, then adjusting that quotient (in seconds) downward until an integer number of time steps occurs each hour. The fourth layer was selected as the critical layer because there are two thicker layers above with faster wind speeds and three thinner layers below with slower wind speeds. Some secondary diffusion still occurs, but the effect is minimized through use of a concentration threshold value. Until the mass of pollutant inside a block increases, via emissions or diffusion into the block, to the

mass corresponding to the concentration threshold value, the diffusion algorithm is skipped for that block. This increases computation efficiency without decreasing prediction accuracy, because the diffusion of concentrations three or four orders of magnitude less than the field maximum is essentially noise.

CHAPTER III

SENSITIVITY TESTING

The diffusion wind atmospheric dispersion model contains a number of modeling options; in this chapter alternatives are tested for their effect upon dispersion results. There are not enough observed data to show which of two modeling alternatives is more accurate, but the options which are most critical for results can be identified.

The first three modeling options examined depict physical processes of pollutant removal. These include surface reflection vs. deposition in section A, fallout vs. no fallout in section B, and chemical transformation vs. a chemically inert pollutant in section C. None of these options appears to greatly affect Tulsa results for values tested.

The addition of a seventh layer to the top of the model in section D showed no effect upon results. The same conclusion would not hold if more layers were created by subdividing some of the current lower and middle layers.

The ambient temperature is demonstrated in section E to have little effect upon plume rise computation and resulting layer assignment, because the major Tulsa industrial sources tend to be relatively hot compared to the range of

ambient temperatures for Tulsa. However, the choice of plume rise formula is shown in section F to be extremely critical in dispersion from elevated industrial sources. Holland's formula always predicts a lower plume rise than Briggs' formula and this leads to higher pollution concentration predictions.

Wind speed and wind direction are found to have more effect upon pollution dispersion from elevated point sources than does stability for the ranges tested. In large part this is due to the stability cases being neutral vs. stable night/unstable day. The daily average of the latter case was probably close to neutral.

In section H the optional meteorological treatments are compared. In general, one would use the best available meteorological data, but the tests demonstrate the importance of accurate prediction of temporal and spatial wind variations.

In section I, the day of the week is shown to be most important for traffic-related pollutants. Examination of source types in section J serves mainly to identify traffic as the most important source of hydrocarbons in Tulsa.

A. Reflection vs. Deposition at the Surface

One of the options in the diffusion wind model is whether to allow deposition of pollution at the surface or to cause pollution to be reflected from that surface. Deposition is not just a process of the pollutant falling onto the ground. The whole process of absorption by plants, buildings, earth,

and human lungs can be included in the parameterization of diffusion, since (from the viewpoint of the dispersion modeler) the important aspect is how much pollutant leaves the atmosphere, and not the exact manner of removal.

Modeling of surface deposition or reflection is accomplished by the treatment of the bottom wall of translated pollution block clouds which are in the surface layer. If the wall position after a diffusion time step is located under the surface (as far as the model is concerned), then the ratio of the depth under the surface to the total cloud depth is the percentage of pollutant mass within that cloud which can be deposited during that time step. The spatial distribution of pollutant mass deposited can be calculated and stored, if desired. An example of calculated deposition is shown in Figure 5. If the bottom wall is repositioned at the surface after translation but before the allocation algorithm, then all of the pollutant mass is again above the surface and reflection is modeled.

Deposition leads to the maximum surface concentration being less and being located closer to the source. Examples of surface concentrations computed with and without deposition are shown in Figures 6a-d. The deposition in Figure 5 occurs under the dispersion situation depicted in Figure 6a.

In Figure 6 and other contoured pollution concentration fields, circled values indicate observed concentrations

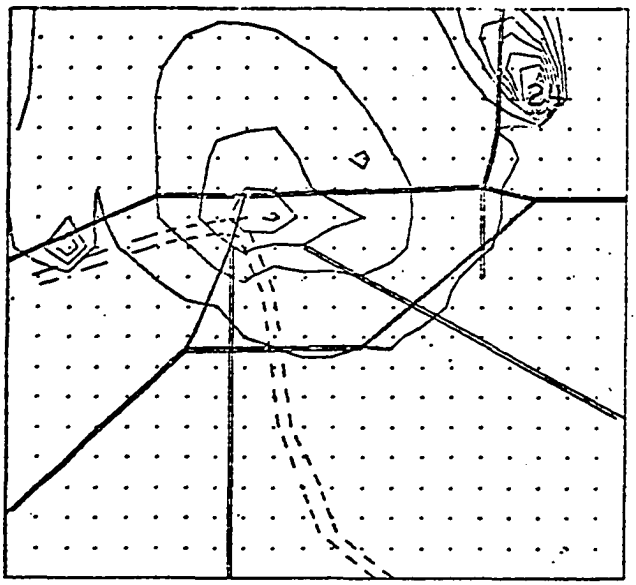

Figure 5: Surface deposition of particulates.

(to be discussed in Chapter IV). The non-circled value in each concentration field is the maximum predicted value. All concentrations shown in this work are for the surface layer. The twenty-four hour resultant surface wind is shown in degrees and meters/second, the average wind speed is shown in meters/second, and the sunshine is expressed as the ratio of sunshine occurring to sunshine possible with clear skies. The minimum contour and the contour interval are given for each concentration pattern.

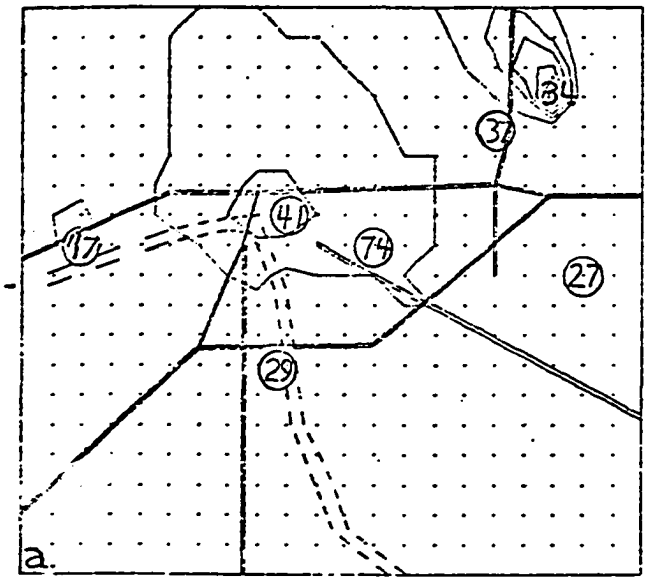

PARTICULATE 24-HR AVG 10 SEPT 74 ALL SOURCES
HOLLAND DEPOSITION 3-HRLY OBS
RESULTANT WIND 145/5.2 AVG SPD 5.5 SUNSHINE 0.17
LOW CONTOUR VALUE=5.0 CONTOUR INTERVAL=5.0
CONCENTRATION IN MICROGRAMS PER CUBIC METER

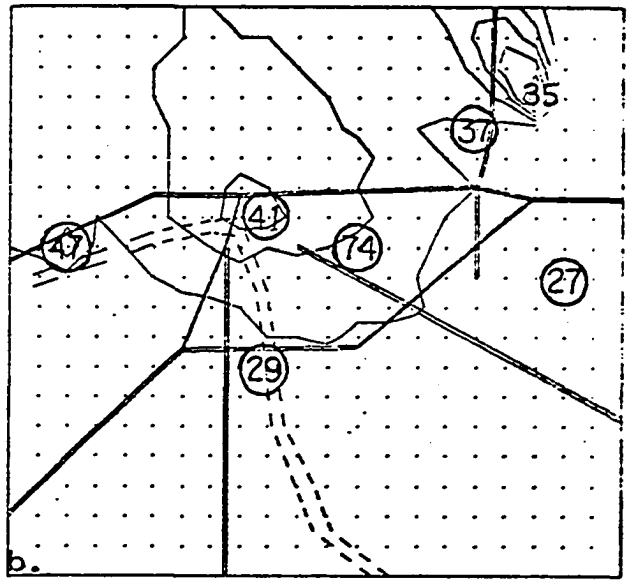

PARTICULATE 24-HR AVG 10 SEPT 74 ALL SOURCES
HOLLAND REFLECTION 3-HRLY OBS
RESULTANT WIND 145/5.2 AVG SPD 5.5 SUNSHINE 0.17
LOW CONTOUR VALUE=5.0 CONTOUR INTERVAL=5.0
CONCENTRATION IN MICROGRAMS PER CUBIC METER

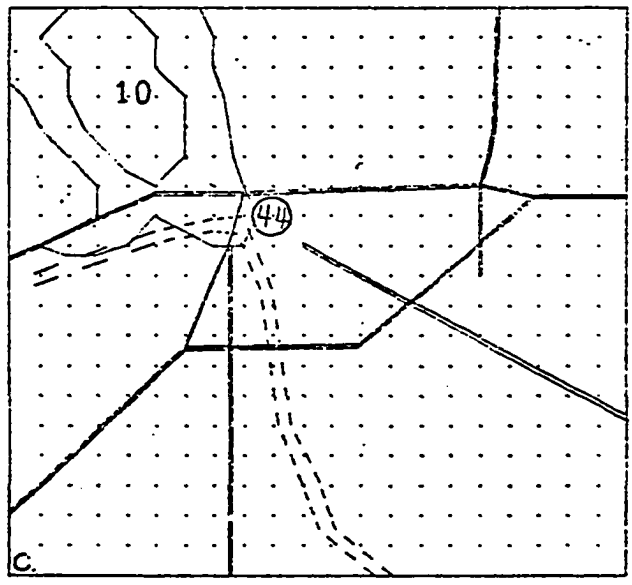

SO2 24-HR AVG 10 SEPT 74 ALL SOURCES
HOLLAND DEPOSITION 3-HRLY OBS
RESULTANT WIND 145/5.2 AVG SPD 5.5 SUNSHINE 0.17
LOW CONTOUR VALUE=5.0 CONTOUR INTERVAL=5.0
CONCENTRATION IN MICROGRAMS PER CUBIC METER

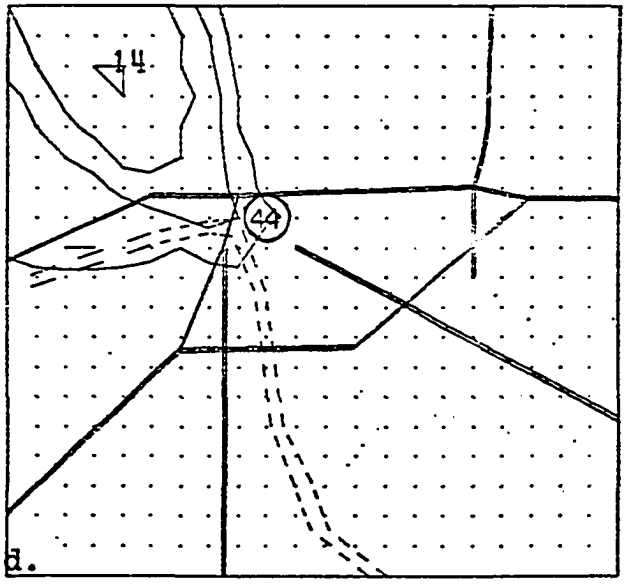

SO2 24-HR AVG 10 SEPT 74 ALL SOURCES
HOLLAND REFLECTION 3-HRLY OBS
RESULTANT WIND 145/5.2 AVG SPD 5.5 SUNSHINE 0.17
LOW CONTOUR VALUE=5.0 CONTOUR INTERVAL=3.0
CONCENTRATION IN MICROGRAMS PER CUBIC METER

Figure 6: Comparison of concentrations resulting from surface deposition vs. surface reflection.

B. Fallout

Fallout of pollutant is simply modeled by adding a downward bias to the translation of the top and bottom of pollution clouds. If the regular wind field is three-dimensional (if a w component is programmed), the fall speed acts as a bias on the vertical wind component. In the simulation of meso-scale dispersion of a cloud of radioactive particles (Shannon, 1974) fall speed varied with both layer and particle size. Layers were five kilometers thick, resulting in a considerable decrease in air density upward through the model layers, while particle size varied from 40 to 300 microns. Fall speed variations are not modeled for the Tulsa urban area because of the shallow model depth (usually 315 meters) and the lack of information on particulate size distribution. It would be inconsistent to model fall speed without modeling deposition. Examples of surface concentrations computed with and without a pollutant fall speed are shown in Figures 7a and 7b.

C. Chemical Transformation

In previous simulations made with the diffusion wind model involving dispersion of a cloud of radioactive particles (Shannon, 1974), it was necessary to model radioactive decay of the particles. This was accomplished by scaling the pollut-ant mass downward each hour, rather than by scaling the radio-activity directly. The hourly scale factor was computed from a half-life term.

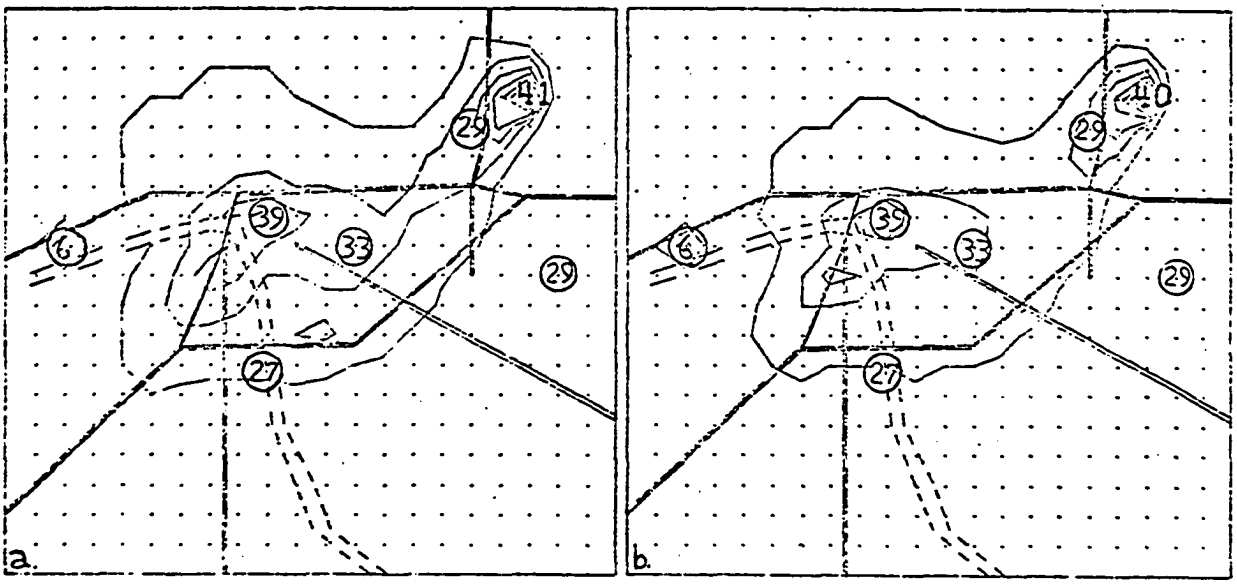

PARTICULATE 24-HR AVG 18 AUG 74 ALL SOURCES
HOLLAND DEPOSITION 3-HRLY OBS FS .1CM/SEC
RESULTANT WIND 104/2.8 AVG SFD 3.8 SUNSHINE 0.65
LOW CONTOUR VALUE=5.0 CONTOUR INTERVAL=5.0
CONCENTRATION IN MICROGRAMS PER CUBIC METER

PARTICULATE 24-HR AVG 18 AUG 74 ALL SOURCES
HOLLAND DEPOSITION 3-HRLY OBS NO FALL SFD
RESULTANT WIND 104/2.8 AVG SFD 3.9 SUNSHINE 0.65
LOW CONTOUR VALUE=5.0 CONTOUR INTERVAL=5.0
CONCENTRATION IN MICROGRAMS PER CUBIC METER

Figure 7: Comparison of particulate concentrations calculated with and without a particle fall speed.

Some of the pollutants modeled for the Tulsa area, particularly nitrogen dioxide and nonmethane hydrocarbons are known to be very active or reactive in the atmosphere. The urban dispersion models which predict smog often have very involved chemical reactions in their programming (Roth, et al., 1974). If a simple approximation, even if a crude approximation, could be found for the effective removal rate of pollutant by chemical transformation, the process could be simulated in the diffusion wind model by an algorithm similar to the radioactive decay algorithm. A comparison of surface concentrations calculated with and without chemical

transformation is shown in Figures 8a and 8b. Half-life for the decay case was arbitrarily set at one hour.

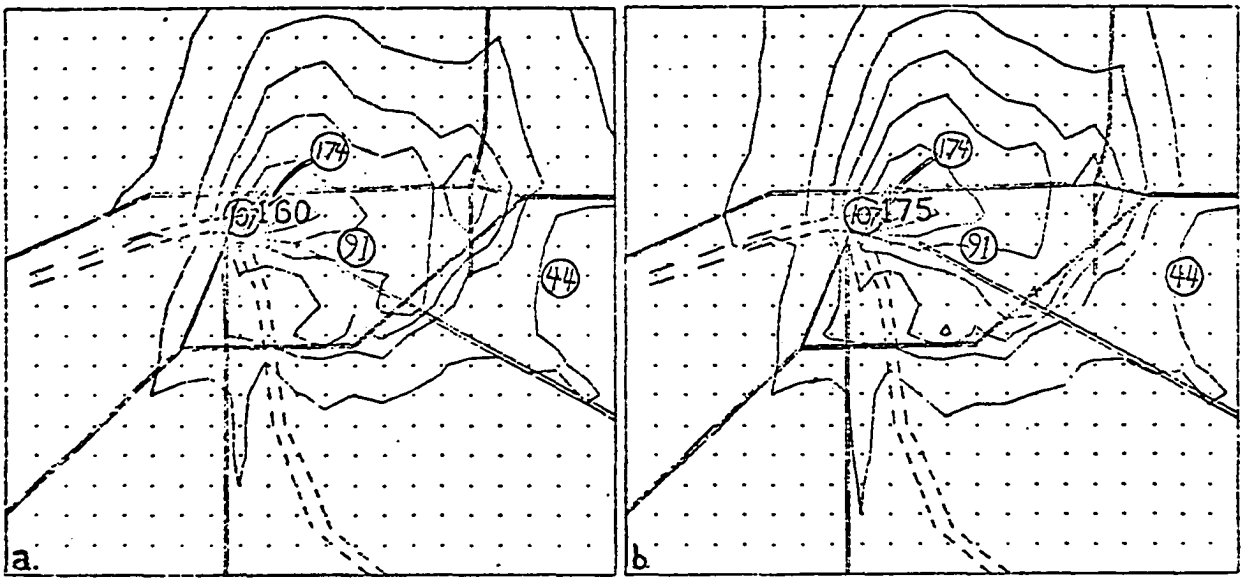

NO2 24-HR AVG 15 JAN 74 ALL SOURCES
HOLLAND DEPOSITION 3-HRLY OBS HL 1HR
RESULTANT WIND 194/3.2 AVG SPD 3.3 SUNSHINE 0.44
LOW CONTOUR VALUE=10.0 CONTOUR INTERVAL=20.0
CONCENTRATION IN MICROGRAMS PER CUBIC METER

NO2 24-HR AVG 15 JAN 74 ALL SOURCES
HOLLAND DEPOSITION 3-HRLY OBS NO DECAY
RESULTANT WIND 194/3.2 AVG SPD 3.3 SUNSHINE 0.44
LOW CONTOUR VALUE=10.0 CONTOUR INTERVAL=20.0
CONCENTRATION IN MICROGRAMS PER CUBIC METER

Figure 8: Comparison of nitrogen dioxide concentrations with a one hour chemical half-life vs. no chemical decomposition.

D. Layer Number and Depth

Early versions of the diffusion wind model contained three layers of depth 400 meters. Deep layers were used because terrain effects led to vertical wind components which were within an order of magnitude of horizontal wind components. Shallow layers would have led to time steps of only a few seconds, and would have made twenty-four hour simulations much more time consuming in computation. The obvious drawback of

the deep layers was the crude vertical resolution, since there were only three values to describe the vertical variation of air pollution concentrations.

The version of the diffusion wind model which was used to simulate dispersion of a cloud of radioactive particles contained eight layers, each of depth five kilometers. This did not cause a problem in prediction of surface concentrations because the modeled cloud was created by a high level source.

In the first adaptation of the model to the Tulsa urban area, five layers of depth 10, 20, 40, 80, and 160 meters were used. This gave reasonable vertical resolution at the surface and total modeled atmospheric depth of 310 meters. Vertical placement of point sources after plume rise was still a bit coarse, since a plume rise to 140 meters left a plume within three layers of the surface, for example. The program was adjusted to allow for as many as ten layers, with depth of each layer as input data. Most simulations were performed using a six layer model (5, 10, 20, 40, 80, and 160 meters depth). The addition of a seventh layer of depth 160 meters made no noticeable difference in surface concentrations on a windy day, as can be noted in Figures 9a and 9b. The additional layer or layers add to computation time. If more layers are used in future applications of the model, it would be better to subdivide the current layers rather than pile more thick layers on top of the modeled atmosphere, as the grid system is too small in horizontal extent for significant interaction between the surface layer and layers above

315 meters except for very low wind speeds.

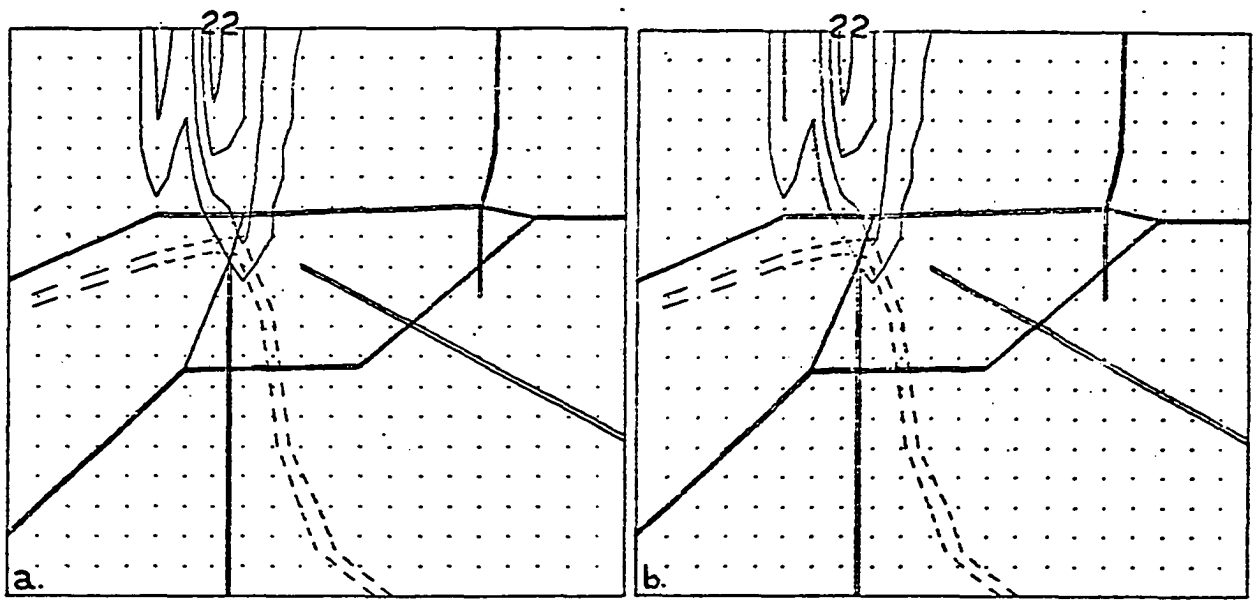

SO2 24-HR AVG 16 JAN 73 ALL SOURCES
HOLLAND DEPOSITION 3-HRLY OBS 7 LAYERS
RESULTANT WIND 184/6.0 AVG SPD 6.1 SUNSHINE 0.37
LOW CONTOUR VALUE=5.0 CONTOUR INTERVAL=5.0
CONCENTRATION IN MICROGRAMS PER CUBIC METER

SO2 24-HR AVG 16 JAN 73 ALL SOURCES
HOLLAND DEPOSITION 3-HRLY OBS 6 LAYERS
RESULTANT WIND 184/6.0 AVG SPD 6.1 SUNSHINE 0.37
LOW CONTOUR VALUE=5.0 CONTOUR INTERVAL=5.0
CONCENTRATION IN MICROGRAMS PER CUBIC METER

Figure 9: Comparison of sulfur dioxide surface concentrations with and without a seventh layer.

E. Ambient Temperature

For most processes of dispersion modeling, surface concentrations are affected not by the ambient temperature directly, but rather by the lapse rate or vertical gradient of temperature. In the computation of plume rise, however, the difference between the stack gas exhaust temperature and the ambient air temperature is a key factor in plume buoyancy, regardless of the particular plume rise formula.

Examination of stack parameters for Tulsa point sources shows that most sources, particularly those sources

in the refinery complex, are relatively hot (575-800°K). Ambient temperatures for Tulsa are generally about 275-300°K. For a stack gas temperature of 600°K, using 275°K instead of 300°K for ambient air temperature results in the temperature difference term changing by about 8%. The resulting change in computed plume rise would be even smaller.

Since Tulsa point source plume rise predictions are relatively insensitive to the ambient temperature, no attempt is made to model ambient temperatures other than by season. Seasonal ambient temperatures, beginning with winter, are 273°K, 288°K, 300°K, and 288°K. Some plume rises computed for SO_2 point sources for winter (season 1) and summer (season 3) are shown in Tables 2a and 2b. The initial layer assignments for the plumes are nearly identical.

F. Plume Rise

The two most widely used formulas for plume rise are those of Holland (1953) and Briggs (1971). Holland's formula was developed from sources with stack diameters from 1.7 to 4.3 meters and stack temperatures from 350 to 577°K (Turner, 1969), while Briggs' formula was developed mainly from the large stacks of power plants.

The formula of Holland is

$$\Delta h = \frac{V_s d}{u} \left(1.5 + 2.68 \times 10^{-3} \, p \, \frac{T_s - T_a}{T_s} \, d\right) \qquad (6)$$

TABLE 2.-- Effect of Ambient Temperature Upon Plume Rise and Layer Apportionment (wind speed is for the surface layer).

HOLLAND PLUME RISE FORMULA

a. WIND SPEED 6.0 METERS PER SECOND P-G STABILITY CLASS D SEASON 1

SOURCE X	SOURCE Y	EMISSION G/SEC	STACK PARAMETERS HGT M	DIAM M	TEMP K	VEL M/SEC	PLUME RISE M	PLUME HGT M	LAYER APPORTIONMENT 1	2	3	4	5	6
8.	12.	8.7	38.1	2.1	660.	9.4	15.1	53.2	0.0	0.0	0.0	1.00	0.0	0.0
8.	12.	1.5	38.1	2.1	721.	3.5	5.8	43.9	0.0	0.0	0.03	0.97	0.0	0.0
8.	12.	0.9	38.1	2.1	778.	2.4	4.2	42.3	0.0	0.0	0.05	0.95	0.0	0.0
8.	12.	0.7	20.4	1.5	788.	5.7	5.7	26.1	0.0	0.0	0.97	0.03	0.0	0.0
8.	12.	4.0	26.5	1.8	723.	4.7	5.8	32.3	0.0	0.0	0.70	0.30	0.0	0.0
8.	12.	2.4	30.2	1.3	723.	5.1	3.9	34.1	0.0	0.0	0.54	0.46	0.0	0.0
8.	12.	6.3	21.3	1.8	880.	9.2	12.1	33.4	0.0	0.0	0.62	0.38	0.0	0.0
8.	12.	2.4	21.6	1.5	736.	4.0	3.9	25.5	0.0	0.0	0.99	0.01	0.0	0.0
8.	12.	0.7	20.4	1.5	714.	5.2	5.0	25.4	0.0	0.0	0.99	0.01	0.0	0.0
8.	12.	1.3	27.7	2.1	623.	4.1	6.3	34.1	0.0	0.0	0.54	0.46	0.0	0.0
8.	12.	3.1	17.7	1.8	739.	3.5	4.6	22.3	0.0	0.05	0.95	0.0	0.0	0.0
8.	12.	2.4	15.5	1.3	723.	5.4	4.1	19.6	0.0	0.17	0.83	0.0	0.0	0.0
8.	12.	110.1	42.7	1.4	800.	7.3	6.1	48.8	0.0	0.0	0.0	1.00	0.0	0.0
8.	12.	16.9	29.0	1.4	723.	6.9	5.6	34.5	0.0	0.0	0.54	0.46	0.0	0.0
8.	12.	0.5	20.4	1.5	811.	4.8	4.8	25.3	0.0	0.0	0.99	0.01	0.0	0.0
8.	12.	0.7	16.2	1.4	533.	3.8	2.7	18.9	0.0	0.23	0.77	0.0	0.0	0.0
8.	12.	8.8	33.8	3.2	578.	3.4	10.2	44.0	0.0	0.0	0.01	0.99	0.0	0.0
8.	12.	1.0	15.2	1.5	578.	9.9	8.1	23.3	0.0	0.03	0.97	0.0	0.0	0.0
8.	12.	23.8	82.3	3.5	578.	2.8	9.8	92.1	0.0	0.0	0.0	0.0	1.00	0.0
8.	12.	5.9	25.9	1.1	578.	15.7	7.9	33.8	0.0	0.0	0.62	0.38	0.0	0.0
8.	12.	5.0	42.7	2.6	717.	11.4	26.5	69.2	0.0	0.0	0.0	0.88	0.12	0.0
9.	11.	7.9	21.3	2.1	430.	10.7	12.8	34.1	0.0	0.0	0.54	0.46	0.0	0.0
9.	11.	5.0	53.3	3.0	711.	3.2	9.7	63.1	0.0	0.0	0.0	1.00	0.0	0.0
9.	11.	1.5	46.0	1.8	625.	3.6	4.2	50.2	0.0	0.0	0.0	1.00	0.0	0.0
9.	11.	5.0	15.2	0.9	708.	1.4	0.6	15.9	0.0	0.46	0.54	0.0	0.0	0.0
9.	11.	0.8	15.2	1.4	767.	1.1	0.9	16.1	0.0	0.38	0.62	0.0	0.0	0.0
9.	11.	0.4	15.2	1.4	717.	1.3	1.1	16.3	0.0	0.38	0.62	0.0	0.0	0.0
9.	11.	1.6	15.2	1.4	717.	1.7	1.4	16.6	0.0	0.38	0.62	0.0	0.0	0.0
9.	11.	0.4	15.2	1.4	678.	1.5	1.2	16.5	0.0	0.38	0.62	0.0	0.0	0.0
9.	11.	0.4	22.9	1.5	678.	1.2	1.2	24.0	0.0	0.01	0.99	0.0	0.0	0.0
9.	11.	2.9	70.7	****	****	0.3	0.0	70.7	0.0	0.0	0.0	0.83	0.17	0.0
9.	11.	1.0	61.0	0.6	578.	2.6	0.6	61.5	0.0	0.0	0.0	1.00	0.0	0.0
10.	10.	0.1	59.1	5.5	444.	27.0	164.2	223.4	0.0	0.0	0.0	0.0	0.0	1.00
6.	12.	48.5	30.5	1.2	343.	8.6	3.6	34.1	0.0	0.0	0.54	0.46	0.0	0.0

b. WIND SPEED 6.0 METERS PER SECOND P-G STABILITY CLASS D SEASON 3

SOURCE X	SOURCE Y	EMISSION G/SEC	STACK PARAMETERS HGT M	DIAM M	TEMP K	VEL M/SEC	PLUME RISE M	PLUME HGT M	LAYER APPORTIONMENT 1	2	3	4	5	6
8.	12.	8.7	38.1	2.1	660.	9.4	14.4	52.5	0.0	0.0	0.0	1.00	0.0	0.0
8.	12.	1.5	38.1	2.1	721.	3.5	5.6	43.7	0.0	0.0	0.03	0.97	0.0	0.0
8.	12.	0.9	38.1	2.1	778.	2.4	4.0	42.1	0.0	0.0	0.05	0.95	0.0	0.0
8.	12.	0.7	20.4	1.5	788.	5.7	5.5	25.9	0.0	0.0	0.99	0.01	0.0	0.0
8.	12.	4.0	26.5	1.8	723.	4.7	5.6	32.1	0.0	0.0	0.70	0.30	0.0	0.0
8.	12.	2.4	30.2	1.3	723.	5.1	3.7	33.9	0.0	0.0	0.62	0.38	0.0	0.0
8.	12.	6.3	21.3	1.8	880.	9.2	11.7	33.1	0.0	0.0	0.62	0.38	0.0	0.0
8.	12.	2.4	21.6	1.5	736.	4.0	3.7	25.4	0.0	0.0	0.99	0.01	0.0	0.0
8.	12.	0.7	20.4	1.5	714.	5.2	4.8	25.2	0.0	0.0	0.99	0.01	0.0	0.0
8.	12.	1.3	27.7	2.1	623.	4.1	6.0	33.7	0.0	0.0	0.62	0.38	0.0	0.0
8.	12.	3.1	17.7	1.8	739.	3.5	4.4	22.1	0.0	0.05	0.95	0.0	0.0	0.0
8.	12.	2.4	15.5	1.3	723.	5.4	3.9	19.5	0.0	0.17	0.83	0.0	0.0	0.0
8.	12.	110.1	42.7	1.4	800.	7.3	5.9	48.6	0.0	0.0	0.0	1.00	0.0	0.0
8.	12.	16.9	29.0	1.4	723.	6.9	5.4	34.3	0.0	0.0	0.54	0.46	0.0	0.0
8.	12.	0.5	20.4	1.5	811.	4.8	4.7	25.1	0.0	0.0	0.99	0.01	0.0	0.0
8.	12.	0.7	16.2	1.4	533.	3.8	2.6	18.7	0.0	0.23	0.77	0.0	0.0	0.0
8.	12.	8.8	33.8	3.2	578.	3.4	9.5	43.4	0.0	0.0	0.03	0.97	0.0	0.0
8.	12.	1.0	15.2	1.5	578.	9.9	7.7	22.9	0.0	0.05	0.95	0.0	0.0	0.0
8.	12.	23.8	82.3	3.5	578.	2.8	9.1	91.4	0.0	0.0	0.0	0.0	1.00	0.0
8.	12.	5.9	25.9	1.1	578.	15.7	7.5	33.5	0.0	0.0	0.62	0.38	0.0	0.0
8.	12.	5.0	42.7	2.6	717.	11.4	25.3	68.0	0.0	0.0	0.0	0.95	0.05	0.0
9.	11.	7.9	21.3	2.1	430.	10.7	11.5	32.9	0.0	0.0	0.70	0.30	0.0	0.0
9.	11.	5.0	53.3	3.0	711.	3.2	9.3	62.6	0.0	0.0	0.0	1.00	0.0	0.0
9.	11.	1.5	46.0	1.8	625.	3.6	4.0	50.0	0.0	0.0	0.0	1.00	0.0	0.0
9.	11.	5.0	15.2	0.9	708.	1.4	0.6	15.8	0.0	0.46	0.54	0.0	0.0	0.0
9.	11.	0.8	15.2	1.4	767.	1.1	0.9	16.1	0.0	0.38	0.62	0.0	0.0	0.0
9.	11.	0.4	15.2	1.4	717.	1.3	1.0	16.3	0.0	0.38	0.62	0.0	0.0	0.0
9.	11.	1.6	15.2	1.4	717.	1.7	1.3	16.6	0.0	0.38	0.62	0.0	0.0	0.0
9.	11.	0.4	15.2	1.4	678.	1.5	1.2	16.4	0.0	0.38	0.62	0.0	0.0	0.0
9.	11.	0.4	22.9	1.5	678.	1.2	1.1	24.0	0.0	0.03	0.97	0.0	0.0	0.0
9.	11.	2.9	70.7	****	****	0.3	0.0	70.7	0.0	0.0	0.0	0.83	0.17	0.0
9.	11.	1.0	61.0	0.6	578.	2.6	0.6	61.5	0.0	0.0	0.0	1.00	0.0	0.0
10.	10.	0.1	59.1	5.5	444.	27.0	143.9	203.1	0.0	0.0	0.0	0.0	0.0	1.00
6.	12.	48.5	30.5	1.2	343.	8.6	3.2	33.7	0.0	0.0	0.62	0.38	0.0	0.0

where Δh is the plume rise in meters,

V_s is the stack gas exhaust velocity (m/sec),

d is the stack diameter (m),

u is the wind speed at stack height (m/sec),

p is the pressure (mb),

T_s is the stack gas temperature (°K), and

T_a is the ambient air temperature (°K).

The plume rise computed from Holland's formula is scaled by a factor which varies from .80 (very stable) to 1.20 (very unstable), as recommended in Turner (1969).

The formula of Briggs is

$$\Delta H = \frac{C(3.5X^*)^{2/3}F^{1/3}}{u} \qquad (7)$$

$$F = g\, V_s\, r_s^2 (T_s - T_a) T_s,$$

$$X^* = 14F^{5/8} \text{ if } F \leq 55,$$

$$X^* = 34F^{2/5} \text{ if } F > 55,$$

where g is the acceleration due to gravity (m/sec^2),

r_s is the stack radius (m),

and C is a constant [C=1.6 in the CDM model; in the TVA models, C is a function of stability and varies from 1.04 (stable) to 1.60 (unstable)].

When Briggs' formula was used in the diffusion wind model, C varied from 1.70 (very unstable) to 1.20 (very stable).

A comparison of plume rise of significant Tulsa

point sources of sulfur dioxide, computed from the formulas of Holland and Briggs, is shown in Tables 3a-3b. The differences in the calculated plume rises are accentuated by the low wind speed. It is noteworthy that the considerably greater rise computed from Briggs' formula leads to the plume rising above the modeled atmosphere (depth 315 meters) in some cases when wind speed is low.

Using expected emission rates and the meteorology of a particular day (January 16, 1973), sensitivity tests were run showing the effect of plume rise formula upon twenty-four hour average surface concentrations. Contoured results are shown in Figures 10a and 10b. Since Holland's plume rise formula gives a lower plume rise for the Tulsa point sources, the resulting concentrations for comparable tests are always higher than when using Brigg's formula.

A comparison of the plume rise formulas, with a bit of manipulation, shows that they have a buoyancy factor in common, defined as $B = V_s d^2 (T_s - T_a)/T_s$. For plumes with low buoyancy ($F \leq 55$), Briggs' formula become

$$\Delta H_b = \frac{C(3.5*14)^{2/3}(9.8/4)^{\cdot 75} B^{\cdot 75}}{u} , \qquad (8)$$

while for sources with large buoyancy ($F > 55$), Briggs' formula becomes

$$\Delta H_b = \frac{C(3.5*34)^{2/3}(9.8/4)^{\cdot 6} B^{\cdot 6}}{u} . \qquad (9)$$

TABLE 3.--Comparison of Plume Rise and Layer Apportionment Resulting From Use of Formulas of Holland (a) and Briggs (b).

HOLLAND PLUME RISE FORMULA

WIND SPEED 2.0 METERS PER SECOND P-G STABILITY CLASS D SEASON 1

SOURCE		EMISSION	STACK PARAMETERS HGT	DIAM	TEMP	VEL	PLUME RISE	PLUME HGT	LAYER APPORTIONMENT					
X	Y	G/SEC	M	M	K	M/SEC	M	M	1	2	3	4	5	6
8.	12.	8.7	38.1	2.1	660.	9.4	45.4	83.5	0.0	0.0	0.0	0.03	0.97	0.0
8.	12.	1.5	38.1	2.1	721.	3.5	17.4	55.5	0.0	0.0	0.0	1.00	0.0	0.0
8.	12.	0.9	38.1	2.1	778.	2.4	12.5	50.6	0.0	0.0	0.0	1.00	0.0	0.0
8.	12.	0.7	20.4	1.5	788.	5.7	17.1	37.5	0.0	0.0	0.30	0.70	0.0	0.0
8.	12.	4.0	26.5	1.8	723.	4.7	17.4	44.0	0.0	0.0	0.03	0.97	0.0	0.0
8.	12.	2.4	30.2	1.3	723.	5.1	11.6	41.8	0.0	0.0	0.08	0.92	0.0	0.0
8.	12.	6.3	21.3	1.8	880.	9.2	36.3	57.7	0.0	0.0	0.0	1.00	0.0	0.0
8.	12.	2.4	21.6	1.5	736.	4.0	11.6	33.3	0.0	0.0	0.62	0.38	0.0	0.0
8.	12.	0.7	20.4	1.5	714.	5.2	15.0	35.4	0.0	0.0	0.46	0.54	0.0	0.0
8.	12.	1.3	27.7	2.1	623.	4.1	19.0	46.8	0.0	0.0	0.0	1.00	0.0	0.0
8.	12.	3.1	17.7	1.8	739.	3.5	13.9	31.6	0.0	0.0	0.77	0.23	0.0	0.0
8.	12.	2.4	15.5	1.3	723.	5.4	12.2	27.7	0.0	0.0	0.95	0.05	0.0	0.0
8.	12.	110.1	42.7	1.4	800.	7.3	18.4	61.1	0.0	0.0	0.0	1.00	0.0	0.0
8.	12.	16.9	29.0	1.4	723.	6.9	16.8	45.7	0.0	0.0	0.0	1.00	0.0	0.0
8.	12.	0.5	20.4	1.5	811.	4.8	14.5	34.9	0.0	0.0	0.54	0.46	0.0	0.0
8.	12.	0.7	16.2	1.4	533.	3.8	8.1	24.3	0.0	0.01	0.99	0.0	0.0	0.0
8.	12.	8.8	33.8	3.2	578.	3.4	30.6	64.5	0.0	0.0	0.0	1.00	0.0	0.0
8.	12.	1.0	15.2	1.5	578.	9.9	24.3	39.5	0.0	0.0	0.17	0.83	0.0	0.0
8.	12.	23.8	82.3	3.5	578.	2.8	29.3	111.6	0.0	0.0	0.0	0.0	1.00	0.0
8.	12.	5.9	25.9	1.1	578.	15.7	23.7	49.6	0.0	0.0	0.0	1.00	0.0	0.0
8.	12.	5.0	42.7	2.6	717.	11.4	79.5	122.1	0.0	0.0	0.0	0.0	1.00	0.0
9.	11.	7.9	21.3	2.1	430.	10.7	38.3	59.6	0.0	0.0	0.0	1.00	0.0	0.0
9.	11.	5.0	53.3	3.0	711.	3.2	29.2	82.6	0.0	0.0	0.0	0.05	0.95	0.0
9.	11.	1.5	46.0	1.8	625.	3.6	12.5	58.5	0.0	0.0	0.0	1.00	0.0	0.0
9.	11.	5.0	15.2	0.9	708.	1.4	1.9	17.1	0.0	0.30	0.70	0.0	0.0	0.0
9.	11.	0.8	15.2	1.4	767.	1.1	2.7	18.0	0.0	0.30	0.70	0.0	0.0	0.0
9.	11.	0.4	15.2	1.4	717.	1.3	3.2	18.4	0.0	0.23	0.77	0.0	0.0	0.0
9.	11.	1.6	15.2	1.4	717.	1.7	4.2	19.4	0.0	0.17	0.83	0.0	0.0	0.0
9.	11.	0.4	15.2	1.4	678.	1.5	3.7	18.9	0.0	0.23	0.77	0.0	0.0	0.0
9.	11.	0.4	22.9	1.5	678.	1.2	3.5	26.4	0.0	0.0	0.97	0.03	0.0	0.0
9.	11.	2.9	70.7	****	****	0.3	0.0	70.7	0.0	0.0	0.0	0.83	0.17	0.0
9.	11.	1.0	61.0	0.6	578.	2.6	1.8	62.7	0.0	0.0	0.0	1.00	0.0	0.0
10.	10.	0.1	59.1	5.5	444.	27.0	492.7	551.8	0.0	0.0	0.0	0.0	0.0	0.0
6.	12.	48.5	30.5	1.2	343.	8.6	10.8	41.3	0.0	0.0	0.08	0.92	0.0	0.0

BRIGGS PLUME RISE FORMULA

WIND SPEED 2.0 METERS PER SECOND P-G STABILITY CLASS D SEASON 1

SOURCE		EMISSION	STACK PARAMETERS HGT	DIAM	TEMP	VEL	PLUME RISE	PLUME HGT	LAYER APPORTIONMENT					
X	Y	G/SEC	M	M	K	M/SEC	M	M	1	2	3	4	5	6
8.	12.	8.7	38.1	2.1	660.	9.4	200.6	238.6	0.0	0.0	0.0	0.0	0.0	1.00
8.	12.	1.5	38.1	2.1	721.	3.5	101.6	139.7	0.0	0.0	0.0	0.0	1.00	0.0
8.	12.	0.9	38.1	2.1	778.	2.4	80.0	118.1	0.0	0.0	0.0	0.0	1.00	0.0
8.	12.	0.7	20.4	1.5	788.	5.7	93.2	113.6	0.0	0.0	0.0	0.0	1.00	0.0
8.	12.	4.0	26.5	1.8	723.	4.7	97.3	123.8	0.0	0.0	0.0	0.0	1.00	0.0
8.	12.	2.4	30.2	1.3	723.	5.1	65.9	96.1	0.0	0.0	0.0	0.0	1.00	0.0
8.	12.	6.3	21.3	1.8	880.	9.2	173.1	194.4	0.0	0.0	0.0	0.0	0.0	1.00
8.	12.	2.4	21.6	1.5	736.	4.0	69.2	90.8	0.0	0.0	0.0	0.0	1.00	0.0
8.	12.	0.7	20.4	1.5	714.	5.2	83.2	103.8	0.0	0.0	0.0	0.0	1.00	0.0
8.	12.	1.3	27.7	2.1	623.	4.1	106.1	133.9	0.0	0.0	0.0	0.0	1.00	0.0
8.	12.	3.1	17.7	1.8	739.	3.5	83.0	100.6	0.0	0.0	0.0	0.0	1.00	0.0
9.	12.	2.4	15.5	1.3	723.	5.4	68.3	83.8	0.0	0.0	0.0	0.03	0.97	0.0
8.	12.	110.1	42.7	1.4	800.	7.3	96.0	138.6	0.0	0.0	0.0	0.0	1.00	0.0
8.	12.	16.9	29.0	1.4	723.	6.9	88.0	117.0	0.0	0.0	0.0	0.0	1.00	0.0
8.	12.	0.5	20.4	1.5	811.	4.8	82.9	103.3	0.0	0.0	0.0	0.0	1.00	0.0
8.	12.	0.7	16.2	1.4	533.	3.8	47.2	63.4	0.0	0.0	0.0	1.00	0.0	0.0
8.	12.	8.8	33.8	3.2	578.	3.4	163.5	197.3	0.0	0.0	0.0	0.0	0.0	1.00
8.	12.	1.0	15.2	1.5	578.	9.9	112.4	127.6	0.0	0.0	0.0	0.0	1.00	0.0
8.	12.	23.8	82.3	3.5	578.	2.8	160.9	243.2	0.0	0.0	0.0	0.0	0.0	1.00
8.	12.	5.9	25.9	1.1	578.	15.7	98.7	124.6	0.0	0.0	0.0	0.0	1.00	0.0
8.	12.	5.0	42.7	2.6	717.	11.4	293.0	335.7	0.0	0.0	0.0	0.0	0.0	0.0
9.	11.	7.9	21.3	2.1	430.	10.7	158.9	180.2	0.0	0.0	0.0	0.0	0.0	1.00
9.	11.	5.0	53.3	3.0	711.	3.2	160.9	214.2	0.0	0.0	0.0	0.0	0.0	1.00
9.	11.	1.5	46.0	1.8	625.	3.6	73.6	119.6	0.0	0.0	0.0	0.0	1.00	0.0
9.	11.	5.0	15.2	0.9	708.	1.4	14.7	29.9	0.0	0.0	0.88	0.12	0.0	0.0
9.	11.	0.8	15.2	1.4	767.	1.1	22.8	38.0	0.0	0.0	0.23	0.77	0.0	0.0
9.	11.	0.4	15.2	1.4	717.	1.3	25.1	40.3	0.0	0.0	0.12	0.88	0.0	0.0
9.	11.	1.6	15.2	1.4	717.	1.7	31.1	46.3	0.0	0.0	0.0	1.00	0.0	0.0
9.	11.	0.4	15.2	1.4	678.	1.5	27.7	43.0	0.0	0.0	0.05	0.95	0.0	0.0
9.	11.	0.4	22.9	1.5	678.	1.2	27.7	50.6	0.0	0.0	0.0	1.00	0.0	0.0
9.	11.	2.9	70.7	****	****	0.3	0.0	70.7	0.0	0.0	0.0	0.83	0.17	0.0
9.	11.	1.0	61.0	0.6	578.	2.6	11.0	72.0	0.0	0.0	0.0	0.77	0.23	0.0
10.	10.	0.1	59.1	5.5	444.	27.0	911.1	970.2	0.0	0.0	0.0	0.0	0.0	0.0
6.	12.	48.5	30.5	1.2	343.	8.6	37.9	68.4	0.0	0.0	0.0	0.92	0.08	0.0

If we assume that the term $T_s/(d^*(T_s-T_a))$ is approximately 1, which is roughly the case for Tulsa sources, and assume neutral stability, Holland's formula becomes

$$\Delta H_h \cong \frac{(1.5+2.5)}{u} B. \tag{10}$$

With constant C set at 1.5 for neutral stability, the ratio of Briggs' plume rise to Holland's plume rise for low buoyancy is approximately

$$\Delta H_b/\Delta H_h \cong 10/B^{.25} \tag{11}$$

while the ratio for high buoyancy is approximately

$$\Delta H_b/\Delta H_h \cong 15/B^{.4} . \tag{12}$$

The most buoyant point source is in block (10, 10), and it can be seen that the associated plume rises are more similar than any other case. The large differences in the two formulas is due mainly to their being developed from different stack parameter and plume rise observation data.

For the same day, surface concentrations resulting from adding biases of 20, 10, -10, and -20 meters to the plume rises computed for each formula are shown in Figures 11a-11h. The effect of a plume rise bias is greater for Holland's formula, since the plume rises predicted by the formula of Holland are lower, but the use of a minimum plume height in the algorithm eases this somewhat.

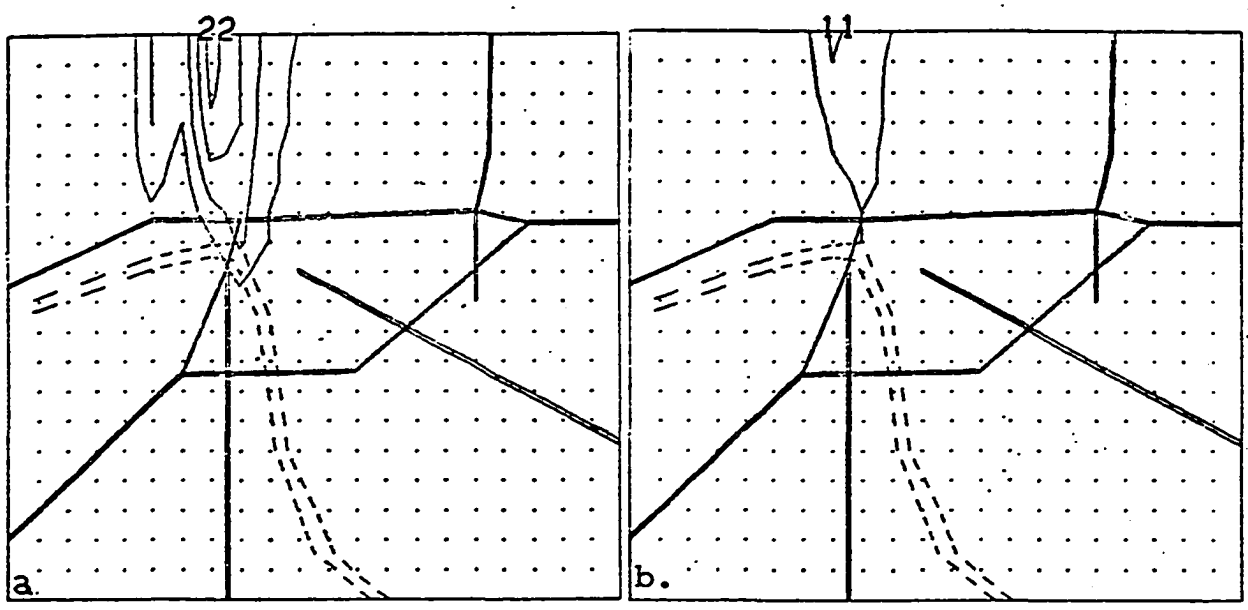

SO2 24-HR AVG 16 JAN 73 ALL SOURCES
HOLLAND DEPOSITION MET VAR ABOUT 3-HR OBS
RESULTANT WIND 184/6.0 AVG SPD 6.1 SUNSHINE 0.37
LOW CONTOUR VALUE=5.0 CONTOUR INTERVAL=5.0
CONCENTRATION IN MICROGRAMS PER CUBIC METER

SO2 24-HR AVG 16 JAN 73 ALL SOURCES
BRIGGS DEPOSITION 3-HRLY OBS
RESULTANT WIND 184/6.0 AVG SPD 6.1 SUNSHINE 0.37
LOW CONTOUR VALUE=5.0 CONTOUR INTERVAL=5.0
CONCENTRATION IN MICROGRAMS PER CUBIC METER

Figure 10: Comparison of sulfur dioxide concentrations for Holland's plume rise equation vs. Briggs' plume rise equation.

The effect upon surface concentrations of doubling or of halving predicted plume rises are shown in Figures 12a-d. Since Briggs' formula predicts higher plume rises, the effects upon surface concentrations of scaling Briggs' predictions are more marked.

The most probable cause of error in operational prediction of plume rise is an inaccurate wind field. Since the predicted plume rise from each formula is inversely proportional to wind speed, an error in the predicted wind is more nearly akin to a scaling error in plume rise prediction.

As a conservative measure, Holland's formula is used in most results of the diffusion wind model which are shown

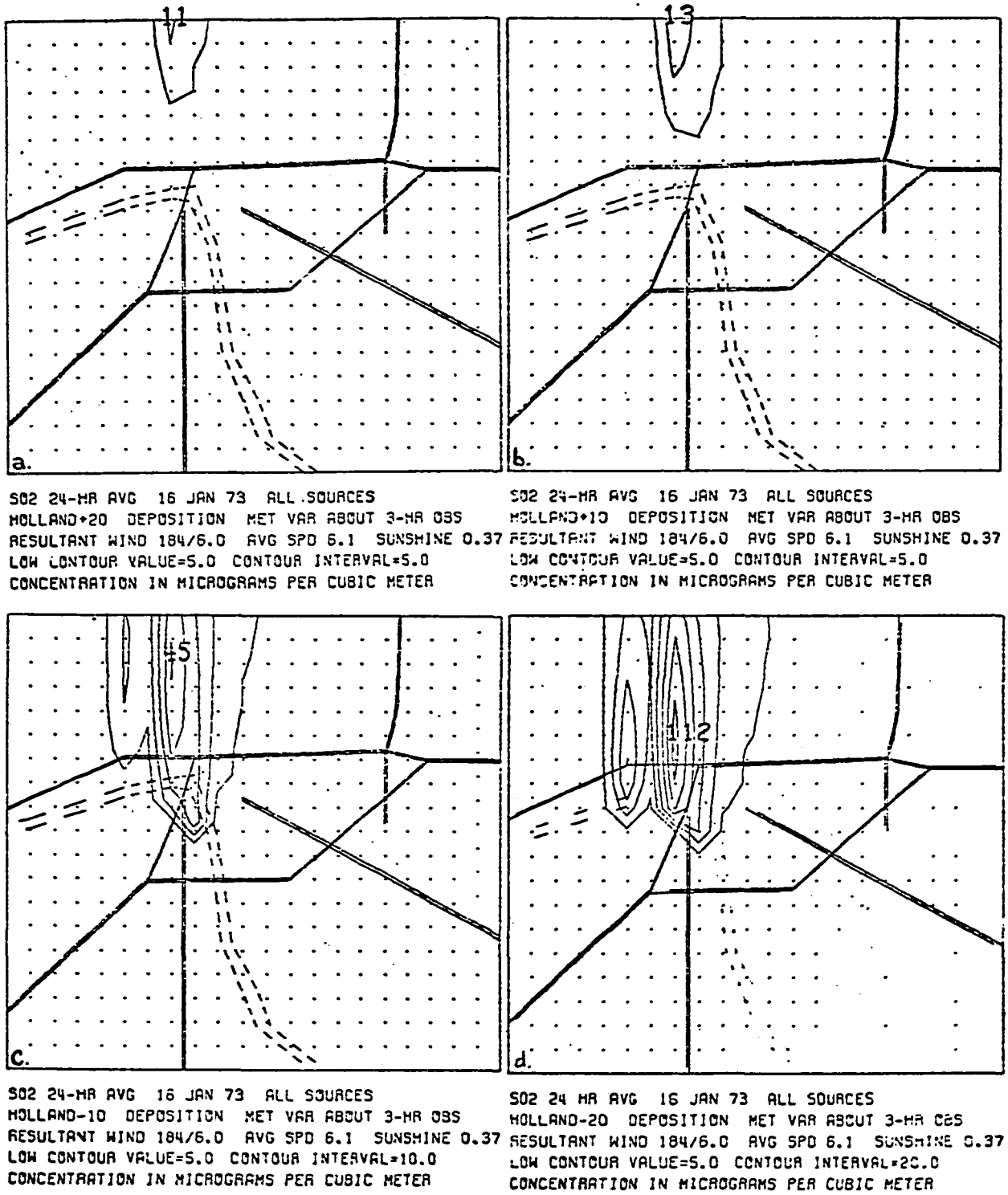

Figure 11: Effect upon surface SO_2 concentrations of a bias (in meters) in predicted plume rise for both Holland's and Briggs' plume rise equation.

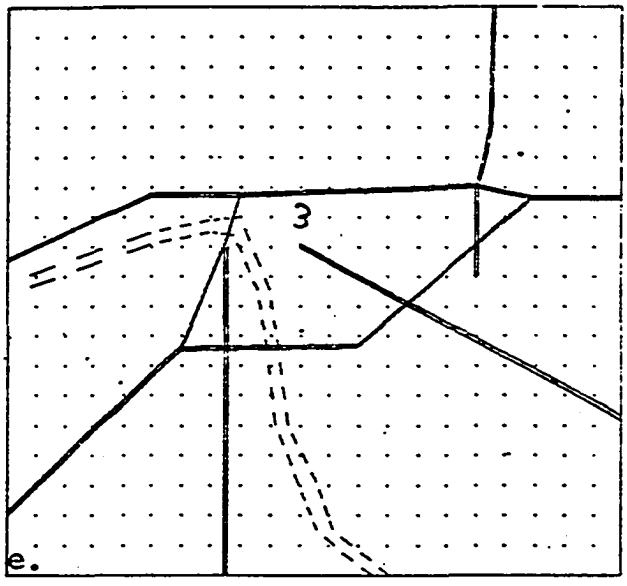

SO2 24-HR AVG 16 JAN 73 ALL SOURCES
BRIGGS+20 DEPOSITION 3-HRLY OBS
RESULTANT WIND 184/6.0 AVG SPD 6.1 SUNSHINE 0.37
LOW CONTOUR VALUE=5.0 CONTOUR INTERVAL=5.0
CONCENTRATION IN MICROGRAMS PER CUBIC METER

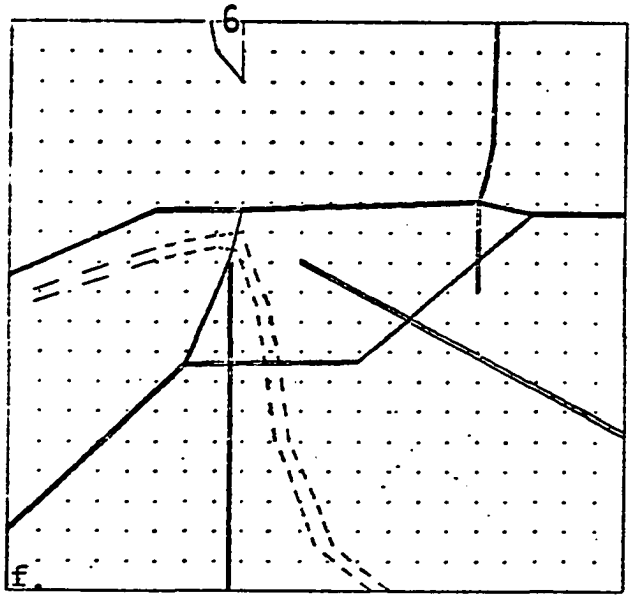

SO2 24-HR AVG 16 JAN 73 ALL SOURCES
BRIGGS+10 DEPOSITION 3-HRLY OBS
RESULTANT WIND 184/6.0 AVG SPD 6.1 SUNSHINE 0.37
LOW CONTOUR VALUE=5.0 CONTOUR INTERVAL=5.0
CONCENTRATION IN MICROGRAMS PER CUBIC METER

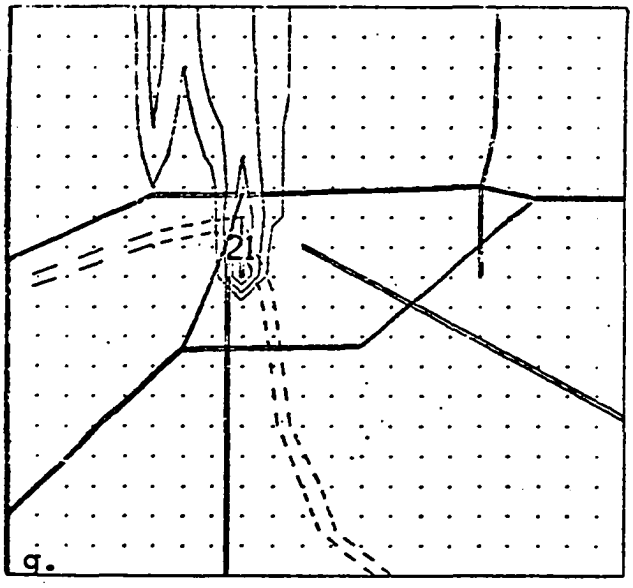

SO2 24-HR AVG 16 JAN 73 ALL SOURCES
BRIGGS-10 DEPOSITION 3-HRLY OBS
RESULTANT WIND 184/6.0 AVG SPD 6.1 SUNSHINE 0.37
LOW CONTOUR VALUE=5.0 CONTOUR INTERVAL=5.0
CONCENTRATION IN MICROGRAMS PER CUBIC METER

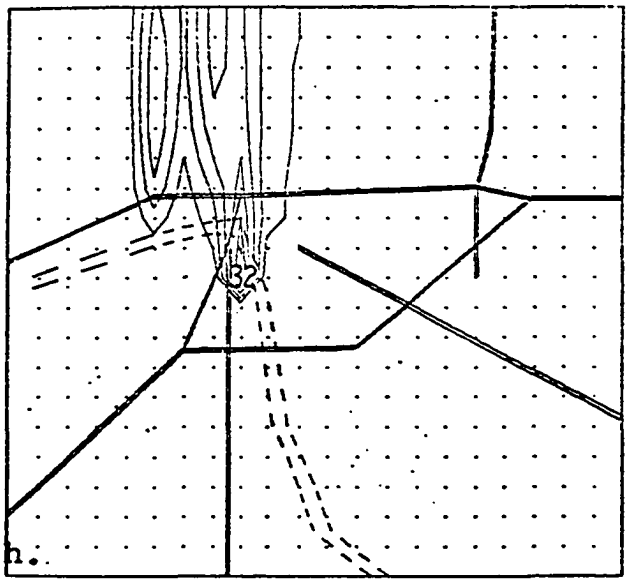

SO2 24-HR AVG 16 JAN 73 ALL SOURCES
BRIGGS-20 DEPOSITION 3-HRLY OBS
RESULTANT WIND 184/6.0 AVG SPD 6.1 SUNSHINE 0.37
LOW CONTOUR VALUE=5.0 CONTOUR INTERVAL=5.0
CONCENTRATION IN MICROGRAMS PER CUBIC METER

Figure 11 (continued).

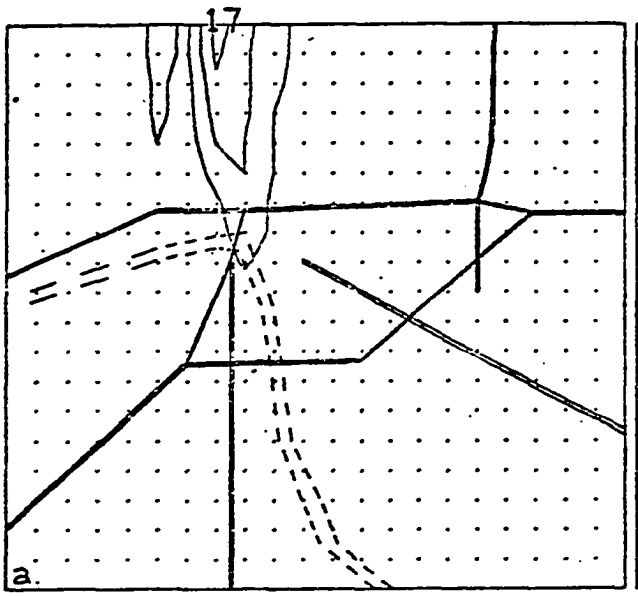

SO2 24-HR AVG 16 JAN 73 ALL SOURCES
HOLLAND=2 DEPOSITION 3-HRLY OBS
RESULTANT WIND 184/6.0 AVG SPD 6.1 SUNSHINE 0.37
LOW CONTOUR VALUE=5.0 CONTOUR INTERVAL=5.0
CONCENTRATION IN MICROGRAMS PER CUBIC METER

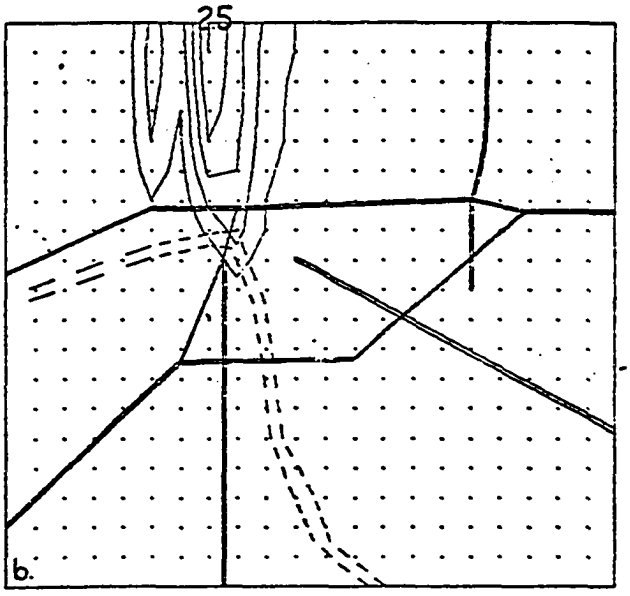

SO2 24-HR AVG 16 JAN 73 ALL SOURCES
HOLLAND=.5 DEPOSITION 3-HRLY OBS
RESULTANT WIND 184/6.0 AVG SPD 6.1 SUNSHINE 0.37
LOW CONTOUR VALUE=5.0 CONTOUR INTERVAL=5.0
CONCENTRATION IN MICROGRAMS PER CUBIC METER

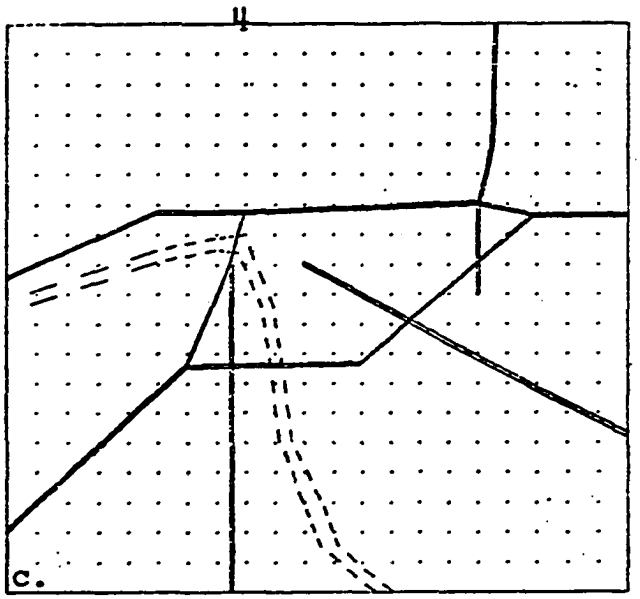

SO2 24-HR AVG 16 JAN 73 ALL SOURCES
BRIGGS=2 DEPOSITION 3-HRLY OBS
RESULTANT WIND 184/6.0 AVG SPD 6.1 SUNSHINE 0.37
LOW CONTOUR VALUE=5.0 CONTOUR INTERVAL=5.0
CONCENTRATION IN MICROGRAMS PER CUBIC METER

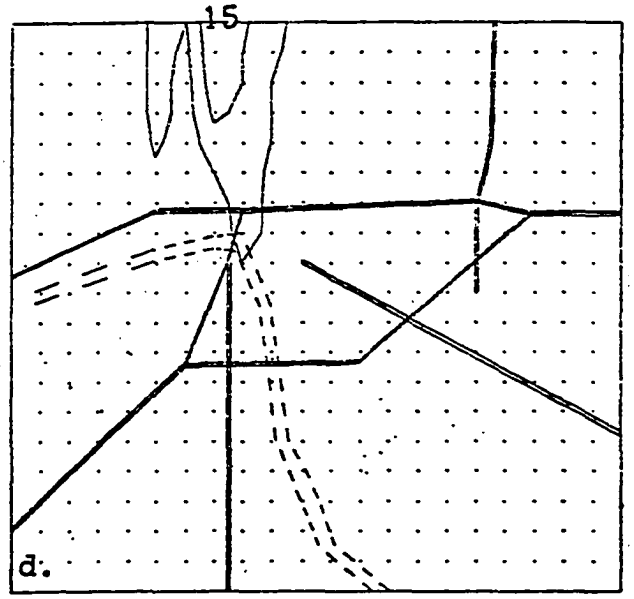

SO2 24-HR AVG 16 JAN 73 ALL SOURCES
BRIGGS=.5 DEPOSITION 3-HRLY OBS
RESULTANT WIND 184/6.0 AVG SPD 6.1 SUNSHINE 0.37
LOW CONTOUR VALUE=5.0 CONTOUR INTERVAL=5.0
CONCENTRATION IN MICROGRAMS PER CUBIC METER

Figure 12: Effect upon surface SO_2 concentrations of scaling plume rise predicted by Holland's and by Briggs' equations by factors of 2 and 1/2.

in Chapters III and IV. Holland's formula was developed from sources most like those of Tulsa.

G. Meteorological Factors

The value of various meteorological factors is second only to emission rates in effect upon the air pollution concentration fields. Some comparison tests were made with one meteorological parameter varied each simulation. The parameters varied were wind speed, wind direction, and percentage of sunshine. The surface concentrations resulting from a light resultant surface wind (1.5 meters/second) and from a strong resultant surface wind (7.5 meters/second) are compared in Figures 13a and 13b. The average wind speed was one meter/second stronger in each instance. The effect upon surface concentrations of a resultant twenty-four hour wind direction perpendicular to the refinery sources (which are oriented generally E-W in the model) and parallel to the refinery sources are shown in Figures 14a and 14b. The effect upon surface concentrations of the daily stability patterns implied by clear skies and by overcast skies are shown in Figures 15a and 15b. In the clear sky case, the strong radiative flux causes daytime instability and nocturnal stability, while overcast skies lead to neutral stability both day and night.

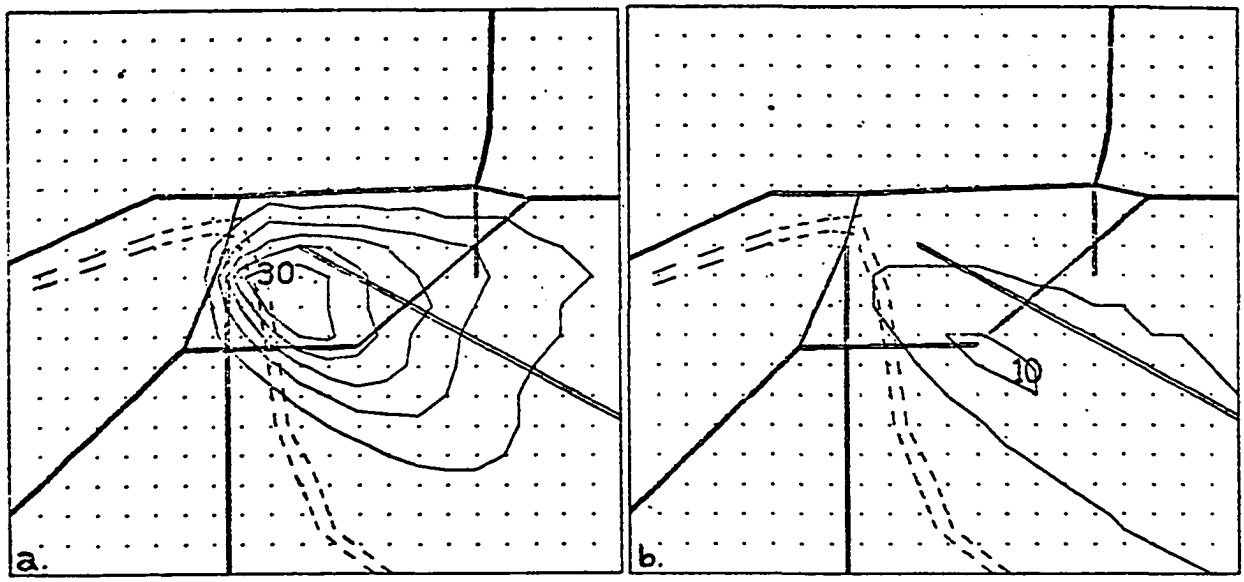

SO2 24-HR AVG ALL SOURCES
HOLLAND DEPOSITION MET VAR ABOUT DAILY MEAN
RESULTANT WIND 300/1.5 AVG SPD 2.5 SUNSHINE 0.50
LOW CONTOUR VALUE=5.0 CONTOUR INTERVAL=5.0
CONCENTRATION IN MICROGRAMS PER CUBIC METER

SO2 24-HR AVG ALL SOURCES
HOLLAND DEPOSITION MET VAR ABOUT DAILY MEAN
RESULTANT WIND 300/7.5 AVG SPD 8.5 SUNSHINE 0.50
LOW CONTOUR VALUE=5.0 CONTOUR INTERVAL=5.0
CONCENTRATION IN MICROGRAMS PER CUBIC METER

Figure 13: Comparison of sulfur dioxide concentrations for light wind speeds vs. strong wind speeds.

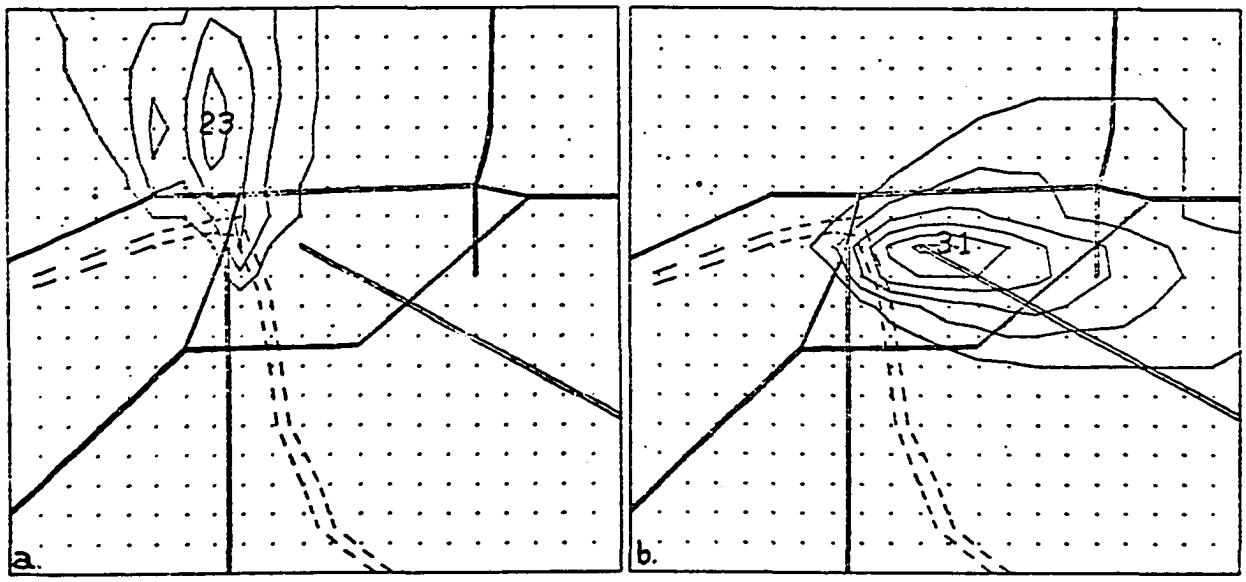

SO2 24-HR AVG ALL SOURCES
HOLLAND DEPOSITION MET VAR ABOUT DAILY MEAN
RESULTANT WIND 180/3.0 AVG SPD 3.0 SUNSHINE 0.50
LOW CONTOUR VALUE=5.0 CONTOUR INTERVAL=5.0
CONCENTRATION IN MICROGRAMS PER CUBIC METER

SO2 24-HR AVG ALL SOURCES
HOLLAND DEPOSITION MET VAR ABOUT DAILY MEAN
RESULTANT WIND 270/3.0 AVG SPD 3.0 SUNSHINE 0.50
LOW CONTOUR VALUE=5.0 CONTOUR INTERVAL=5.0
CONCENTRATION IN MICROGRAMS PER CUBIC METER

Figure 14: Comparison of sulfur dioxide concentrations for wind blowing across sources vs. winds blowing along sources.

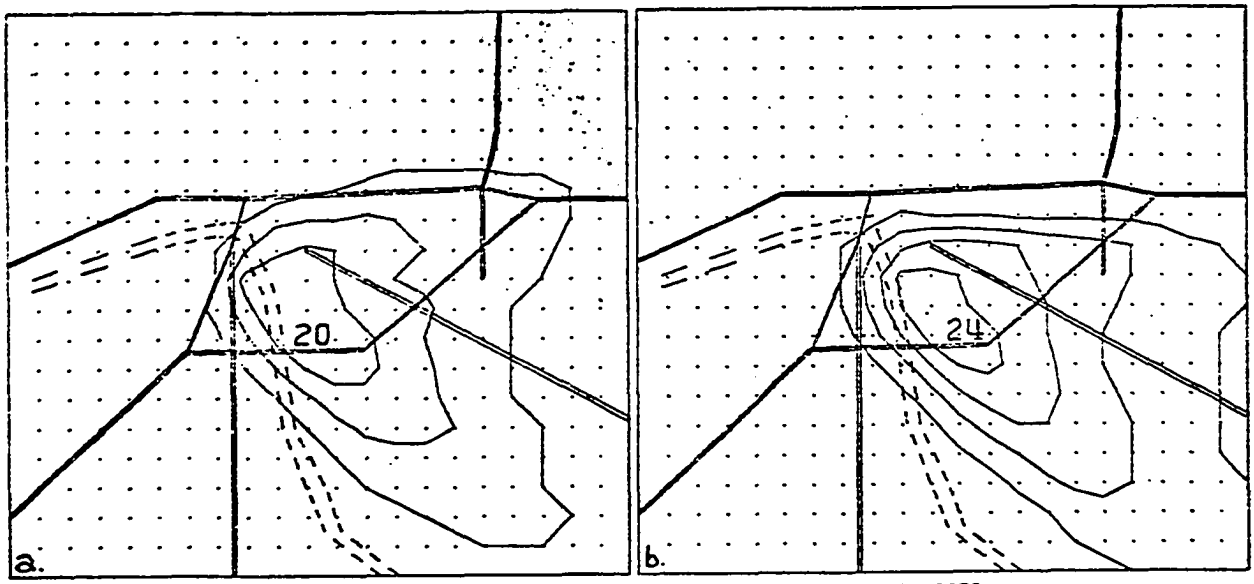

SO2 24-HR AVG ALL SOURCES
HOLLAND DEPOSITION MET VAR ABOUT DAILY MEAN
RESULTANT WIND 300/3.0 AVG SPD 3.0 SUNSHINE 1.00
LOW CONTOUR VALUE=5.0 CONTOUR INTERVAL=5.0
CONCENTRATION IN MICROGRAMS PER CUBIC METER

SO2 24-HR AVG ALL SOURCES
HOLLAND DEPOSITION MET VAR ABOUT DAILY MEAN
RESULTANT WIND 300/3.0 AVG SPD 3.0 SUNSHINE 0.0
LOW CONTOUR VALUE=5.0 CONTOUR INTERVAL=5.0
CONCENTRATION IN MICROGRAMS PER CUBIC METER

Figure 15: Comparison of sulfur dioxide concentrations for clear skies vs. overcast skies.

H. Meteorological Treatment

For meteorology associated with a particular day (August 10, 1972) hourly concentration patterns and the mean daily pattern were obtained using three different meteorological options. (Use of the climate generator would not pertain to a particular day.)

Hourly concentration patterns and daily means are shown in Figures 16a-d for several different blocks using each of the meteorological options. The blocks correspond to the three central circled observations in Figures 17a-c plus a block to the north at the upper edge of the grid. M indicates using mean daily conditions without a temporal variation,

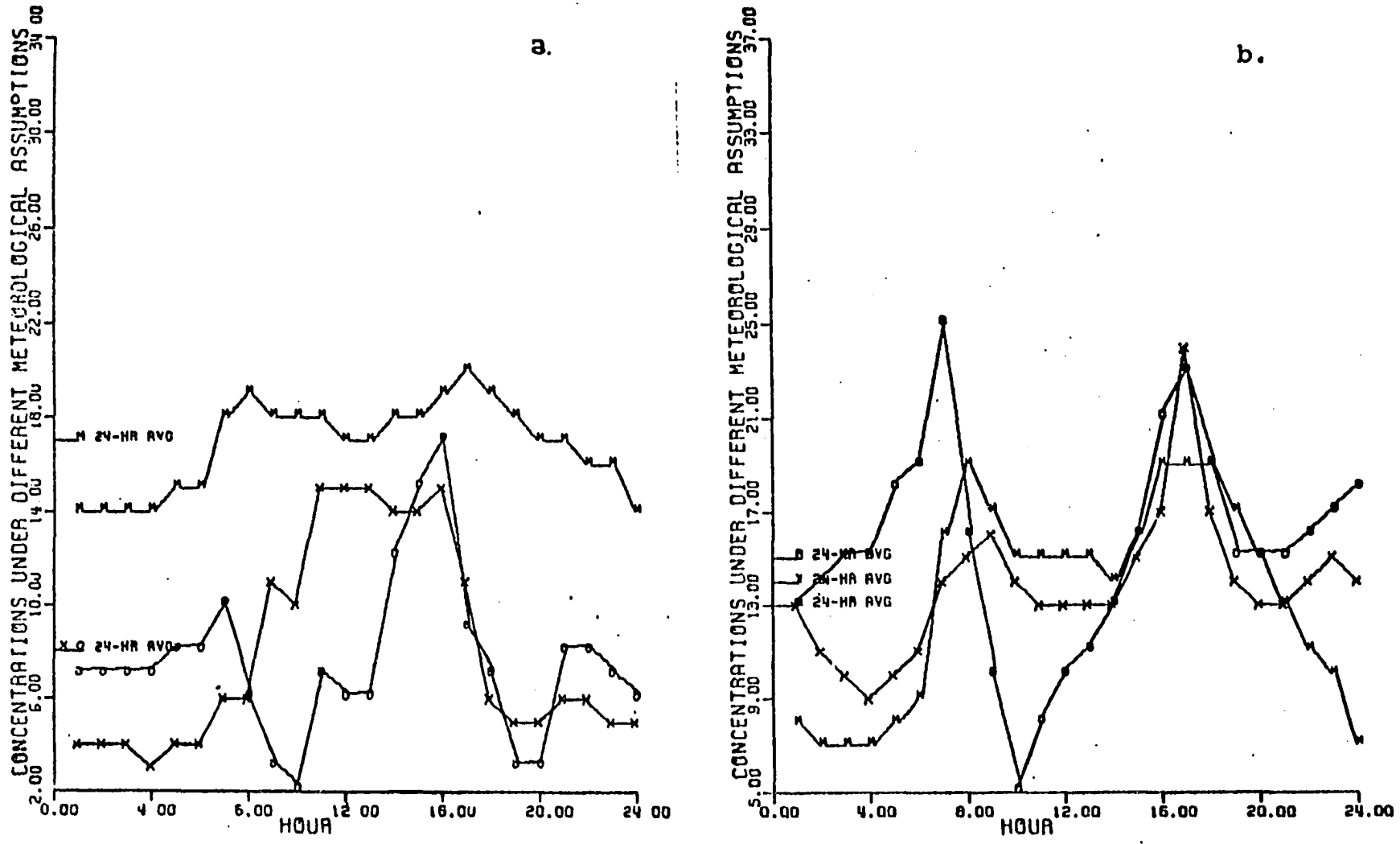

SO2 PREDICTIONS BLOCK(9,11) 15 JAN 74
METEOROLOGICAL TREATMENT: DAILY MEAN(M)
HOURLY VARIATION ABOUT DAILY MEAN(X)
HOURLY VARIATION ABOUT 3-HR OBS(O)

SO2 PREDICTIONS BLOCK(9,13) 15 JAN 74
METEOROLOGICAL TREATMENT: DAILY MEAN(M)
HOURLY VARIATION ABOUT DAILY MEAN(X)
HOURLY VARIATION ABOUT 3-HR OBS(O)

Figure 16: Effect of meteorological treatment upon modeled surface concentrations at various points.

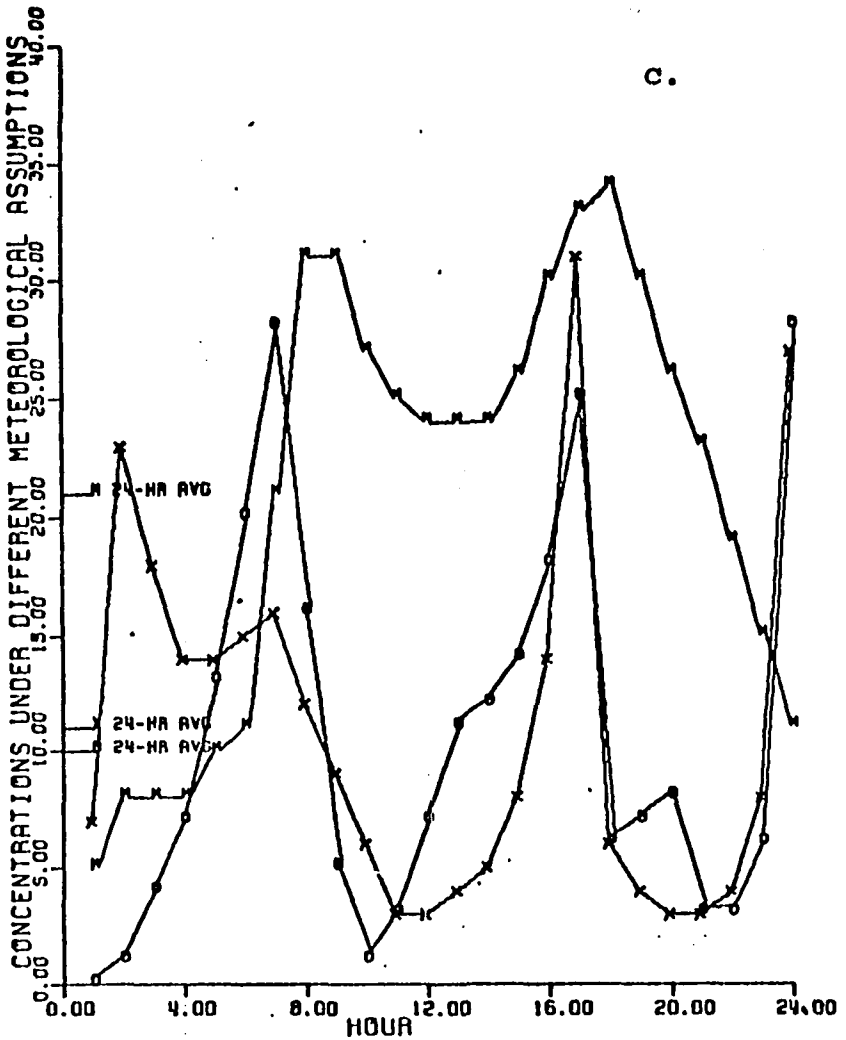

SO2 PREDICTIONS BLOCK(9,20) 15 JAN 74
METEOROLOGICAL TREATMENT: DAILY MEAN(M)
HOURLY VARIATION ABOUT DAILY MEAN(X)
HOURLY VARIATION ABOUT 3-HR OBS(0)

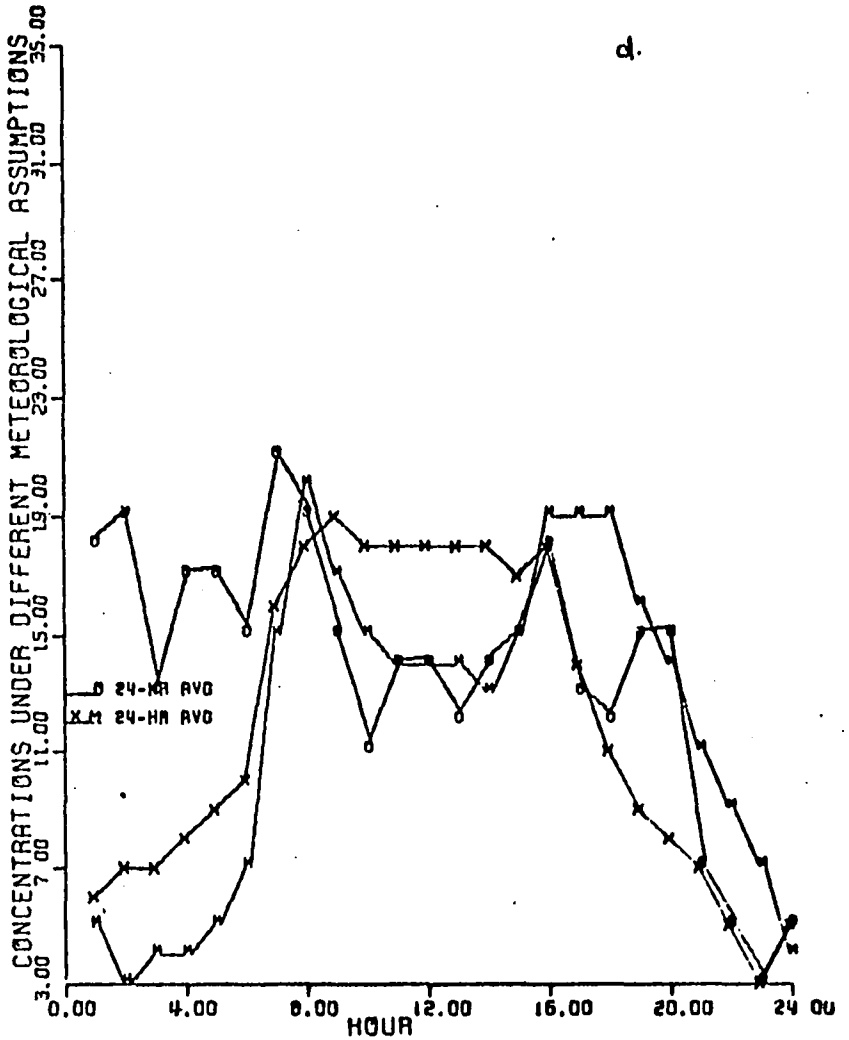

SO2 PREDICTIONS BLOCK(10,13) 15 JAN 74
METEOROLOGICAL TREATMENT: DAILY MEAN(M)
HOURLY VARIATION ABOUT DAILY MEAN(X)
HOURLY VARIATION ABOUT 3-HR OBS(0)

Figure 16 (continued)

X indicates annual average temporal and vertical variations about the daily mean conditions, and 0 indicates use of the three-hourly observations. Emissions are given their normal temporal variations. The spatial pattern of the twenty-four hour average concentrations is shown for each treatment in Figures 17a-c.

The highest maximum concentration was predicted by the use of the time invariant mean daily meteorology, because plume orientation did not vary. If the emissions had been constant in time, the plume would have been more narrow.

There was general agreement between the patterns predicted by the average meteorological variation about the daily mean and the three-hourly observations. This is particularly true for block (9, 20), depicted in Figure 16c, which was the farthest from the major sources.

I. Day of Week

The effect upon industrial emissions of the day of the week is very much a function of the industry. The refineries in the Tulsa area have been essentially continuous sources since the energy and gasoline "crunches" began. On the other hand, the particulate-producing quarries in the northeastern section of the urban area are basically 8-10 hour operations weekdays and in some cases, Saturday.

Traffic and resulting emissions have the familiar double-humped morning and evening rush-hour daily pattern

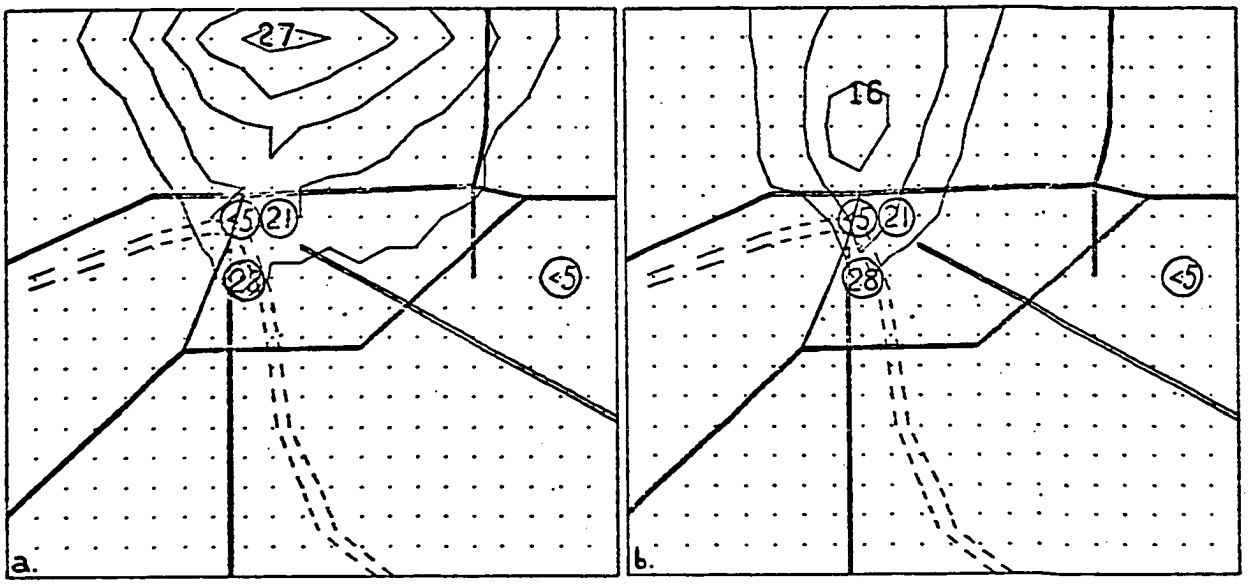

SO2 24-HR AVG 1S JAN 74 ALL SOURCES
HOLLAND DEPOSITION MEAN DAILY MET
RESULTANT WIND 194/3.2 AVG SPD 3.3 SUNSHINE 0.44
LOW CONTOUR VALUE=5.0 CONTOUR INTERVAL=5.0
CONCENTRATION IN MICROGRAMS PER CUBIC METER

SO2 24-HR AVG 1S JAN 74 ALL SOURCES
HOLLAND DEPOSITION VAR ABOUT MEAN DAILY MET
RESULTANT WIND 194/3.2 AVG SPD 3.3 SUNSHINE 0.44
LOW CONTOUR VALUE=5.0 CONTOUR INTERVAL=5.0
CONCENTRATION IN MICROGRAMS PER CUBIC METER

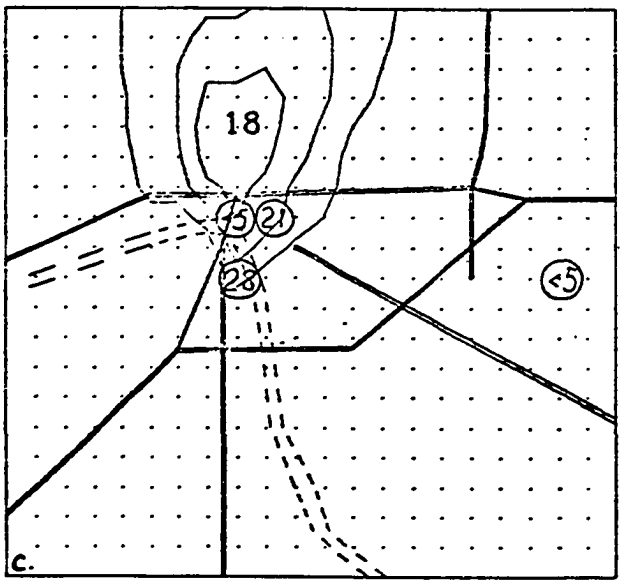

SO2 24-HR AVG 1S JAN 74 ALL SOURCES
HOLLAND DEPOSITION 3-HRLY OBS
RESULTANT WIND 194/3.2 AVG SPD 3.3 SUNSHINE 0.44
LOW CONTOUR VALUE=5.0 CONTOUR INTERVAL=5.0
CONCENTRATION IN MICROGRAMS PER CUBIC METER

Figure 17: Comparison of sulfur dioxide concentrations for different meteorological treatments.

Monday through Friday, while weekend patterns are much harder to define. The fact that much of the weekend traffic is discretionary and recreation-related creates difficulties in predicting an accurate pattern.

The difference in model simulations of dispersion from traffic and service station emissions for a weekday and a Sunday are shown in Figures 18a-18b. The weekday/weekend variation would be greatest for the basic automobile pollutants (NO_2, HC, and CO) and least for SO_2, which is emitted mainly by continuous industrial sources.

J. Source Types

The three source types in the diffusion wind model as applied to Tulsa are industrial sources, mobile sources (traffic), and service stations (hydrocarbons only). Sulfur dioxide and particulates are produced mainly by industrial sources, while nitrogen dioxide, hydrocarbons, and carbon monoxide are mainly the result of traffic. Traffic sources are more general throughout the grid and result in pollution concentration patterns which are less a function of wind direction than in the case of SO_2, which is mainly produced by elevated sources in a small section of the grid. The hydrocarbon concentrations for a given meteorological situation for traffic and service station emissions and for industrial emissions are shown in Figures 18a and 18c, respectively. The cumulative effect is shown in Figure 18d.

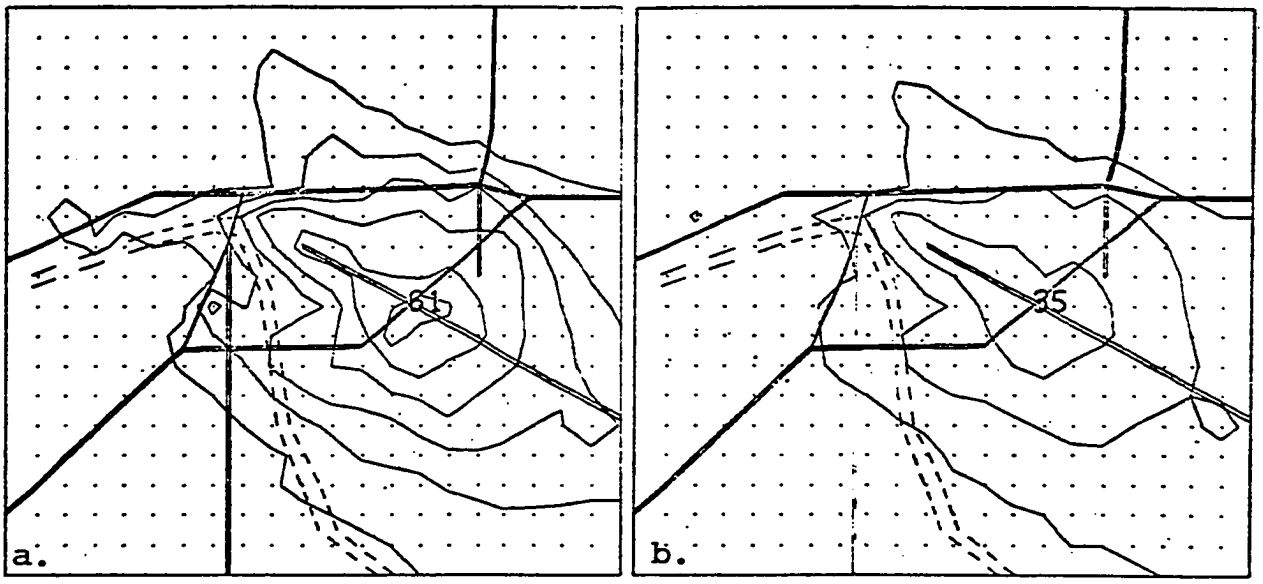

HC 24-HR AVG WEEKDAY TRAFFIC AND S.S.
DEPOSITION NON-METHANE.25 HL 2HRS
RESULTANT WIND 310/4.0 AVG SPD 7.0 SUNSHINE 0.95
LOW CONTOUR VALUE=5.0 CONTOUR INTERVAL=10.0
CONCENTRATION IN MICROGRAMS PER CUBIC METER

HC 24-HR AVG SUNDAY TRAFFIC AND S.S.
DEPOSITION NON-METHANE.25 HL 2HRS
RESULTANT WIND 310/4.0 AVG SPD 7.0 SUNSHINE 0.95
LOW CONTOUR VALUE=5.0 CONTOUR INTERVAL=10.0
CONCENTRATION IN MICROGRAMS PER CUBIC METER

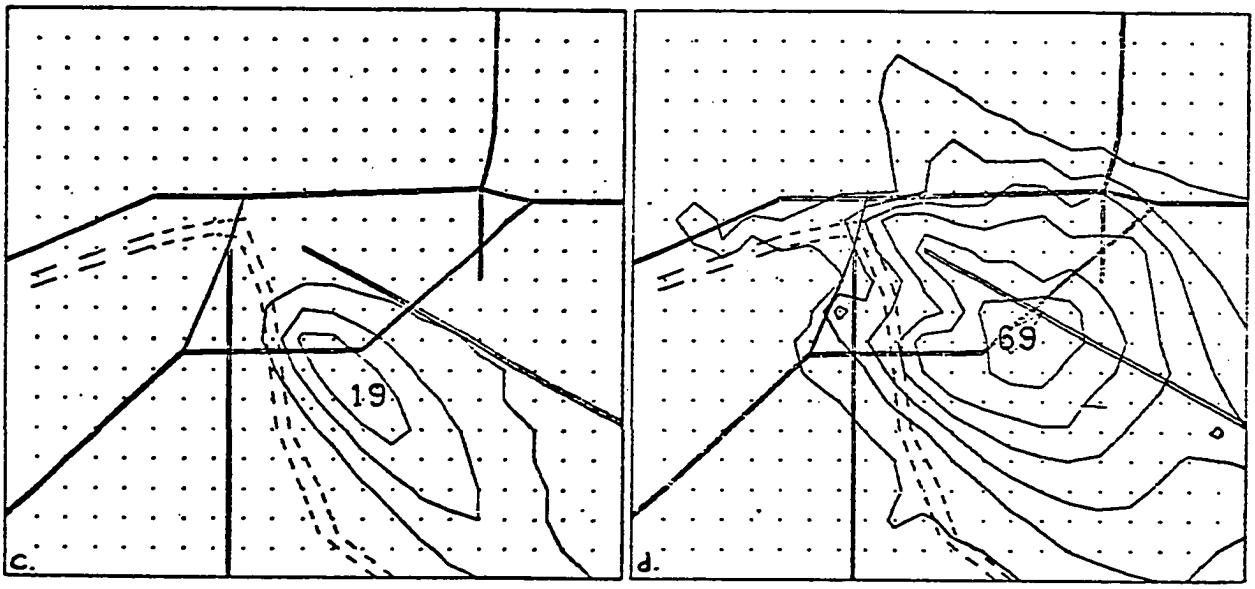

HC 24-HR AVG WEEKDAY INDUSTRIAL
HOLLAND DEPOSITION NON-METHANE.25 HL 2HRS
RESULTANT WIND 310/4.0 AVG SPD 7.0 SUNSHINE 0.95
LOW CONTOUR VALUE=5.0 CONTOUR INTERVAL=5.0
CONCENTRATION IN MICROGRAMS PER CUBIC METER

HC 24-HR AVG WEEKDAY ALL SOURCES
HOLLAND DEPOSITION NON-METHANE.25 HL 2HRS
RESULTANT WIND 310/4.0 AVG SPD 7.0 SUNSHINE 0.95
LOW CONTOUR VALUE=5.0 CONTOUR INTERVAL=10.0
CONCENTRATION IN MICROGRAMS PER CUBIC METER

Figure 18: Effects of the day of the week and type of source upon hydrocarbon concentrations.

CHAPTER IV

COMPARISON TO OBSERVED DATA

A vital part of the calibration and acceptance of dispersion models and other predictive models is comparison of predicted and observed values. It would be ideal to have a great quantity of observed data in both space and time so that statistical statements could be made about the accuracy of the diffusion wind atmospheric dispersion model. During twenty-four hours of dispersion of a pollutant over the Tulsa urban area, the diffusion wind model predicts $22 \times 20 \times 24 = 10,560$ hourly surface concentrations. However, in most cases, there are no observed data to compare with predictions because most measurements of air quality are made only every third day. On the days with observations, there are no more than a half dozen average daily values, and in most cases no more than two or three. The exception to this is carbon monoxide, which has hourly average values at a single point. The complete space/time prediction capability of the diffusion wind atmospheric dispersion model cannot be calibrated by the available air quality data, but some tentative conclusions can be made. Section A contains comparisons of predicted and observed daily averages, while

section B looks at hourly results.

A. Daily Averages

Many of the sensitivity tests involving twenty-four hour average concentrations were made using observed meteorological data on days with air quality measurements. The observed concentrations are shown plotted and circled on the contoured concentration fields, when applicable. The results are also summarized in Table 4.

The most accurate predictions shown in Table 4 are nitrogen dioxide predictions for January 15, 1974. This is true both with and without the half-life factor. Nitrogen dioxide is emitted mainly by widespread traffic sources; thus the resulting patterns are not greatly influenced by wind direction, since there is no single plume to orient. Wind speed and vertical mixing are still quite important, but the most important factor is accuracy of emission inventory. Results indicate that the Tulsa nitrogen dioxide emissions are fairly accurately modeled.

Sulfur dioxide predictions for the same day are not modeled as accurately as nitrogen dioxide. Sulfur dioxide is mainly emitted from elevated point sources. A look at Figure 17 indicates that the wind field may have veered (rotated clockwise) more than the average value predicted by the model. It should also be pointed out that measurements are made at a point, while predictions are square mile averages.

TABLE 4.--Comparison of Observed and Predicted Twenty-four Hour Average Concentrations.

Date	Figure	Pollutant	Observed	Predicted	Option Predicted	
7 Mar 73	22b	SO_2	21	14		
	22a	CO	3.2	1.6		
					half-life 1 hour	
15 Jan 74	8a-b	NO_2	91	93	80	
			174	176	160	
			44	9	7	
			107	118	107	
					mean daily met.	var. about mean daily met.
	17a-c	SO_2	21	13	12	12
			28	8	17	8
			<5	<5	<5	<5
			<5	15	13	14
					fall speed .1 cm/sec.	
18 Aug 74	7a-b	Part.	33	11	13	
			29	1	1	
			39	21	23	
			6	13	13	
			29	13	14	
			27	5	6	
10 Sept 74	6a	Part.	74	7		
			27	1		
			41	15		
			47	12		
			37	3		
			29	2		

(Units micrograms per cubic meter except for CO, which is milligrams per cubic meter. Normal options: Holland plume rise formula, 3-hourly meteorological observations, no fall speed or chemical decay.)

The sulfur dioxide prediction on March 7, 1973 was fairly accurate, but a single observation prevents any inference about spatial accuracy of prediction. The carbon monoxide prediction of the daily average was off by a factor of 2, but again the comparison of a point value to an area average prediction may be the cause. One can nearly always obtain lower carbon monoxide readings by locating the sensor further away from nearby streets.

There seems to be very little accuracy or representativeness in prediction of particulate constructions. This is mostly an emission inventory problem. Many urban particulate sources, such as unpaved roads and construction sites, do not show up in the data. The most inaccurate predictions are those of September 10, which was a windy day. It appears that particulate emission data for Tulsa should contain an area source array which increases emissions with increasing wind speed. Much of this wind dependent emission is dust from such sources as fields, yards, and playgrounds.

B. Hourly Averages

Since hourly observations of carbon monoxide concentrations are available, hourly surface results of the diffusion wind model for the square mile containing the CO sensor are compared with observed values. The daily patterns for March 7, 1973 are shown in Figure 19. It is apparent that the dominant feature is the diurnal traffic pattern, since the major hump is the morning rush hour, when emissions

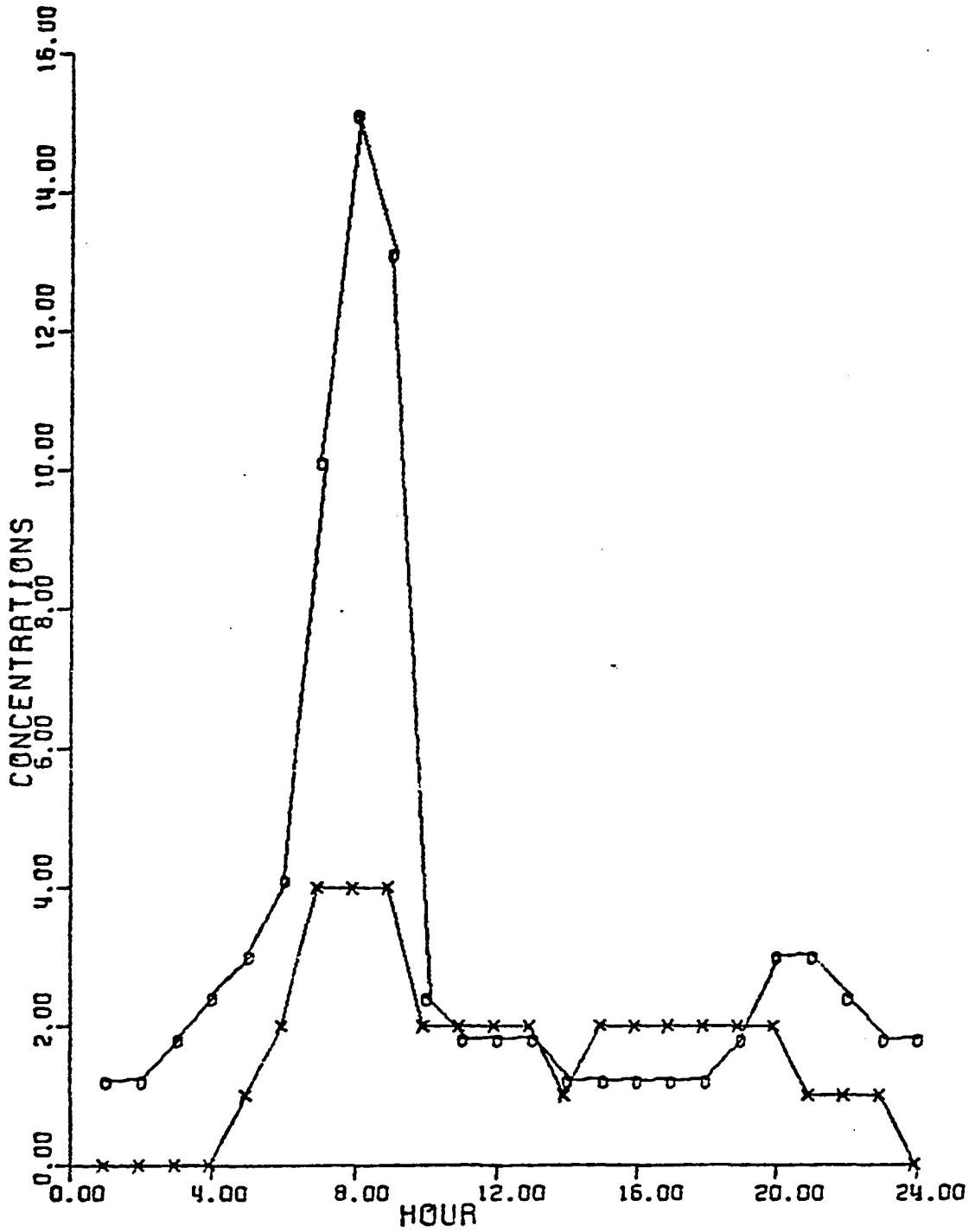

Figure 19: Comparison of predicted vs. observed carbon monoxide hourly concentrations.

are high and dispersion is poor. The evening rush hour is much less marked, even in the modeled results, because dispersion conditions are better. The increase in the morning maximum of the observed concentrations (15 mg/m^3) over that of the modeled concentrations (4 mg/m^3) is due to the fact that the observed concentration is an average at a point near a large line source, while the modeled concentration is a square mile average.

The spatial pattern of the carbon monoxide concentration field is shown at three-hour intervals in Figures 20a-20h. The location of the maximum concentration is not greatly shifted by the wind, since the peak is closely related to the downtown traffic peak, but the general orientation of the CO pattern does shift.

The spatial pattern of the sulfur dioxide concentration field, also for March 7, 1973 is shown at three-hour intervals in Figures 21a-21h. There is only a daily average with which to compare the modeled values, but it is instructive to note the wide variation in some of the hourly concentration patterns from which the daily average pattern is computed. The predicted hourly patterns vary widely with changes in the observed wind. This is due to the sources being basically elevated point sources which are located in a relatively small area of the grid. If the horizontal block dimensions were doubled, the sulfur dioxide sources could almost be combined into a single equivalent source.

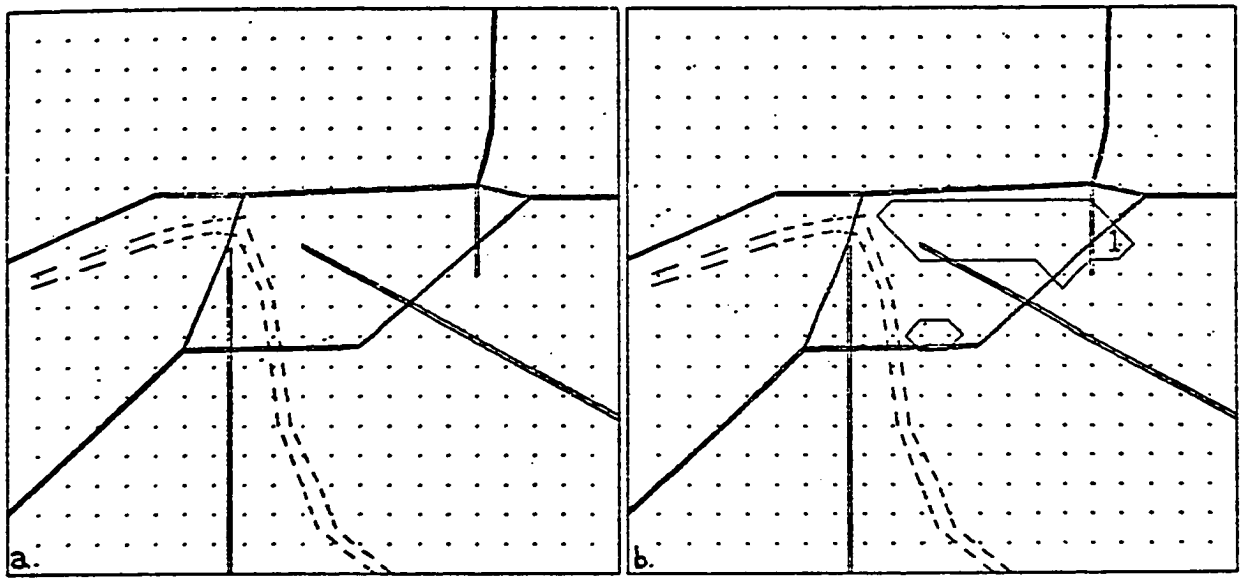

CO HRLY AVG 7 MAR 73 0300 CST
WIND 300/2.1 M/SEC CLEAR
CONCENTRATION IN MILLIGRAMS PER CUBIC METER
LOW CONTOUR VALUE=0.5 CONTOUR INTERVAL=1.0

CO HRLY AVG 7 MAR 73 0600 CST
WIND 250/1.5 M/SEC CLEAR
CONCENTRATION IN MILLIGRAMS PER CUBIC METER
LOW CONTOUR VALUE=0.5 CONTOUR INTERVAL=1.0

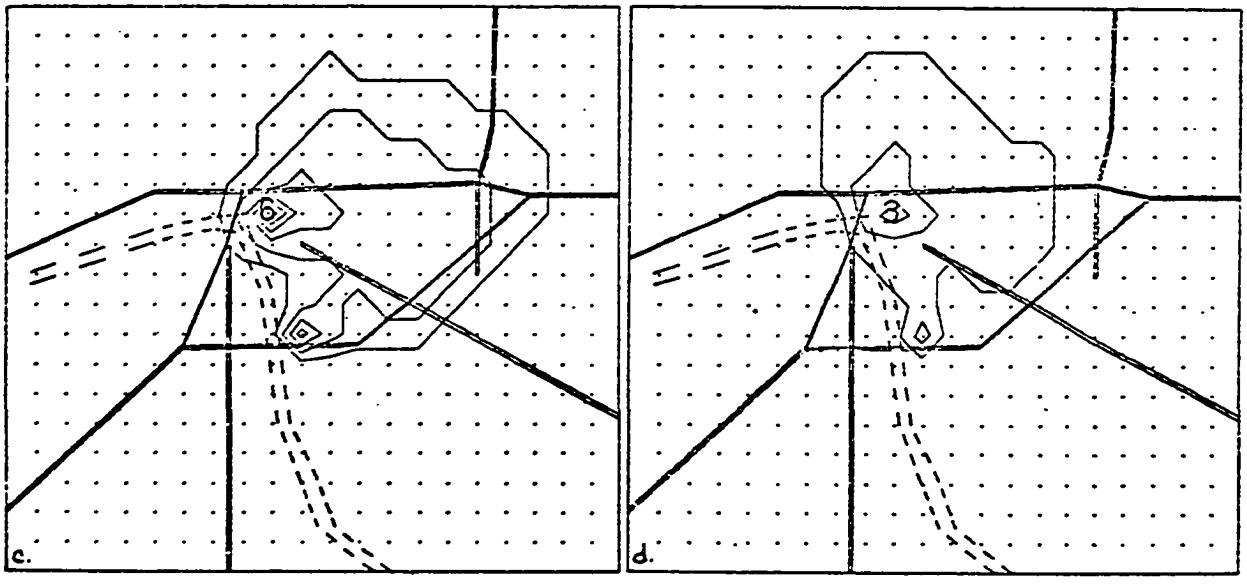

CO HRLY AVG 7 MAR 73 0900 CST
WIND 200/1.5 M/SEC CLEAR
CONCENTRATION IN MILLIGRAMS PER CUBIC METER
LOW CONTOUR VALUE=0.5 CONTOUR INTERVAL=1.0

CO HRLY AVG 7 MAR 73 1200 CST
WIND 150/3.1 M/SEC CLOUD COVER .20
CONCENTRATION IN MILLIGRAMS PER CUBIC METER
LOW CONTOUR VALUE=0.5 CONTOUR INTERVAL=1.0

Figure 20: Hourly carbon monoxide concentrations at three-hourly intervals.

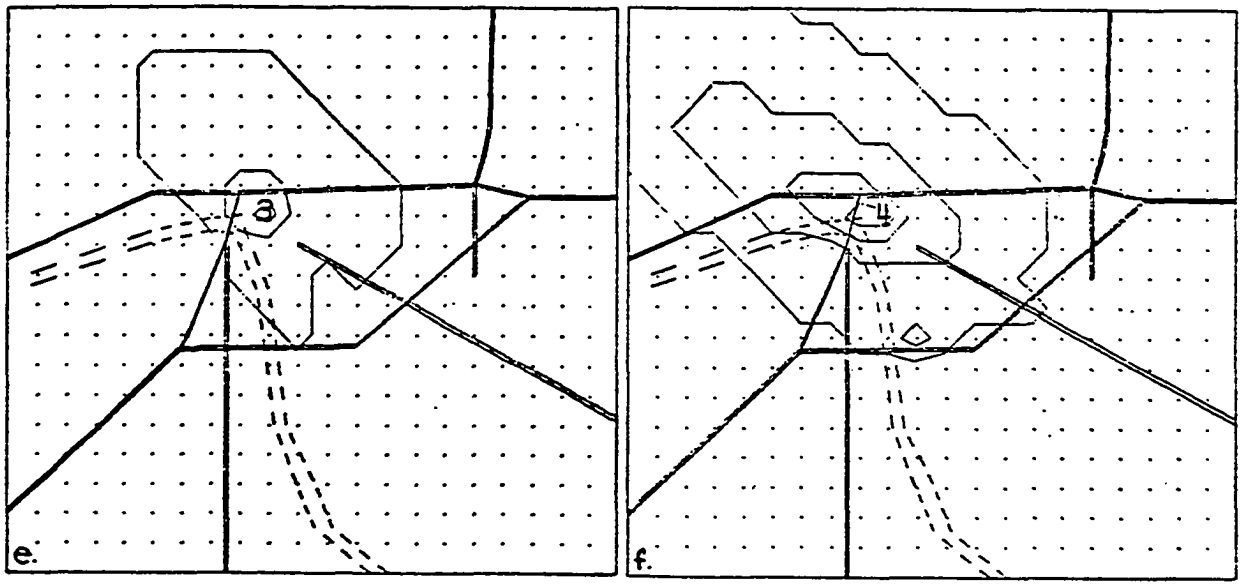

CO HRLY AVG 7 MAR 73 1500 CST
WIND 140/3.1 M/SEC CLOUD COVER .20
CONCENTRATION IN MILLIGRAMS PER CUBIC METER
LOW CONTOUR VALUE=0.5 CONTOUR INTERVAL=1.0

CO HRLY AVG 7 MAR 73 1800 CST
WIND 110/3.6 M/SEC CLOUD COVER .80
CONCENTRATION IN MILLIGRAMS PER CUBIC METER
LOW CONTOUR VALUE=0.5 CONTOUR INTERVAL=1.0

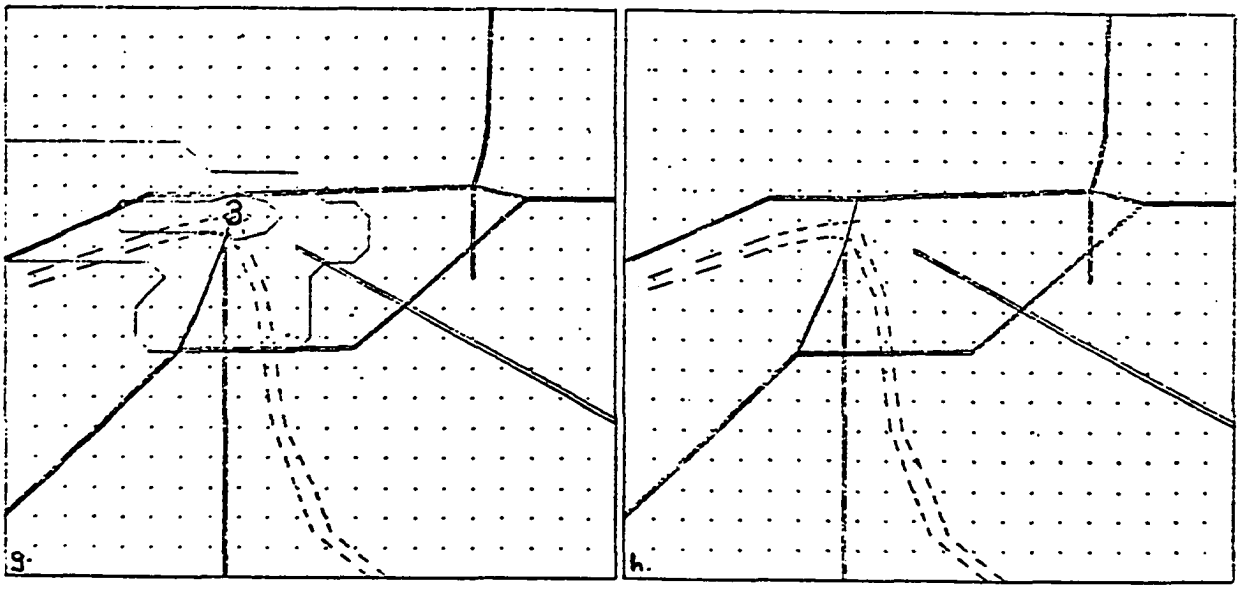

CO HRLY AVG 7 MAR 73 2100 CST
WIND 000/2.6 M/SEC CLOUD COVER .90
CONCENTRATION IN MILLIGRAMS PER CUBIC METER
LOW CONTOUR VALUE=0.5 CONTOUR INTERVAL=1.0

CO HRLY AVG 8 MAR 73 0000 CST
WIND 110/4.1 M/SEC CLOUD COVER .60
CONCENTRATION IN MILLIGRAMS PER CUBIC METER
LOW CONTOUR VALUE=0.5 CONTOUR INTERVAL=1.0

Figure 20 (continued)

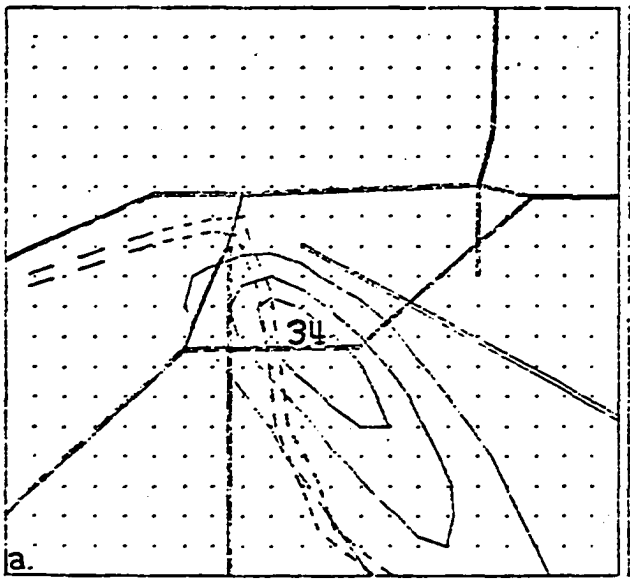

SO2 HRLY AVG 7 MAR 73 0300 CST
WIND 300/2.1 M/SEC CLEAR
CONCENTRATION IN MICROGRAMS PER CUBIC METER
LOW CONTOUR VALUE=5.0 CONTOUR INTERVAL=10.0

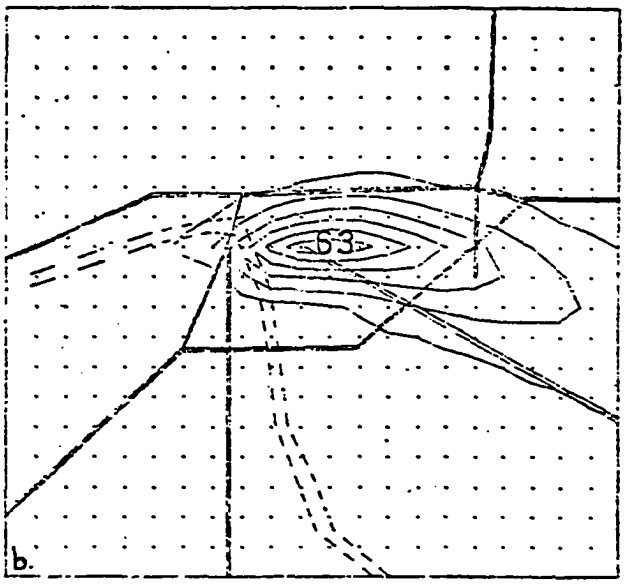

SO2 HRLY AVG 7 MAR 73 0600 CST
WIND 250/1.5 M/SEC CLEAR
CONCENTRATION IN MICROGRAMS PER CUBIC METER
LOW CONTOUR VALUE=5.0 CONTOUR INTERVAL=10.0

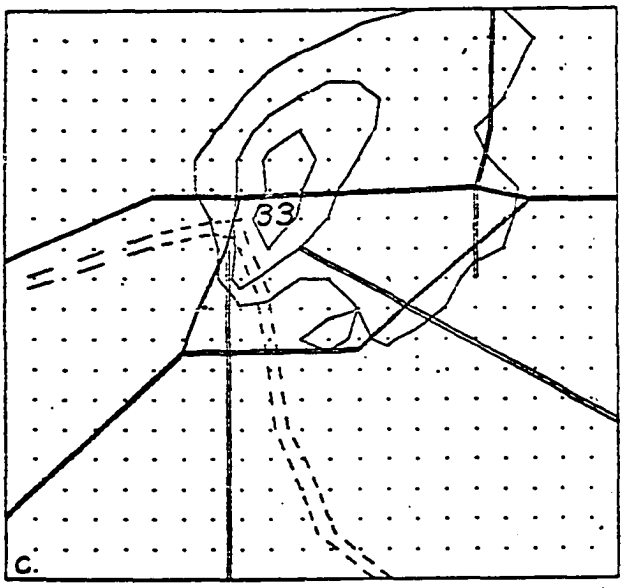

SO2 HRLY AVG 7 MAR 73 0900 CST
WIND 200/1.5 M/SEC CLEAR
CONCENTRATION IN MICROGRAMS PER CUBIC METER
LOW CONTOUR VALUE=5.0 CONTOUR INTERVAL=10.0

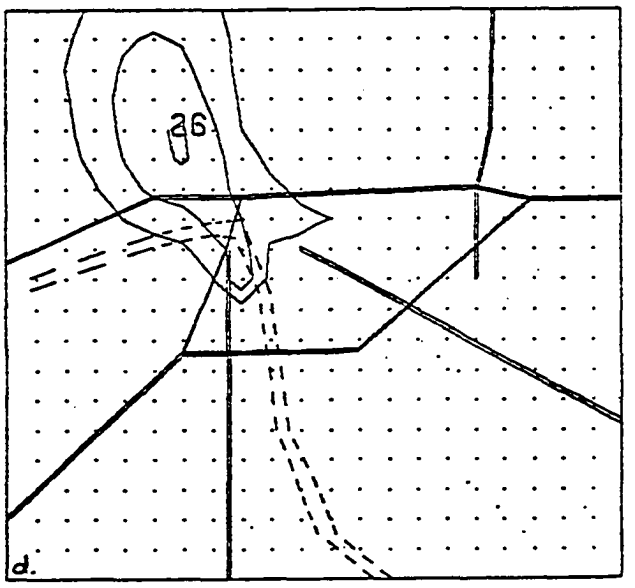

SO2 HRLY AVG 7 MAR 73 1200 CST
WIND 150/3.1 M/SEC CLOUD COVER .20
CONCENTRATION IN MICROGRAMS PER CUBIC METER
LOW CONTOUR VALUE=5.0 CONTOUR INTERVAL=10.0

Figure 21: Hourly sulfur dioxide concentrations at three-hourly intervals.

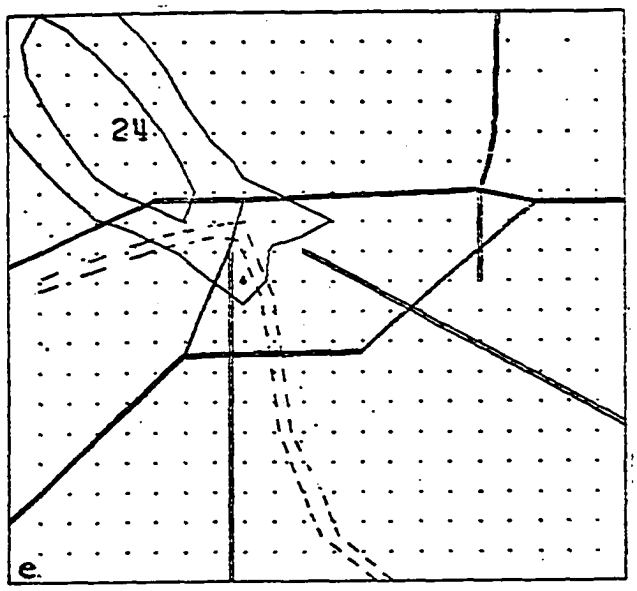

SO2 HRLY AVG 7 MAR 73 1500 CST
WIND 140/3.1 M/SEC CLOUD COVER .20
CONCENTRATION IN MICROGRAMS PER CUBIC METER
LOW CONTOUR VALUE=5.0 CONTOUR INTERVAL=10.0

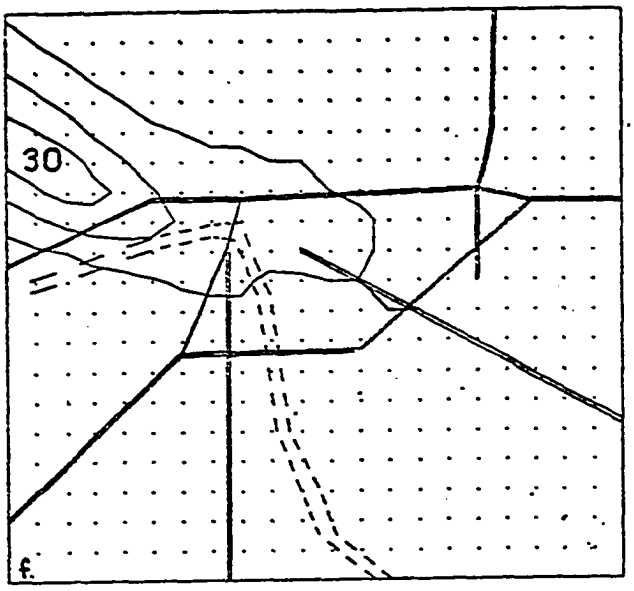

SO2 HRLY AVG 7 MAR 73 1800 CST
WIND 110/3.6 M/SEC CLOUD COVER .80
CONCENTRATION IN MICROGRAMS PER CUBIC METER
LOW CONTOUR VALUE=5.0 CONTOUR INTERVAL=10.0

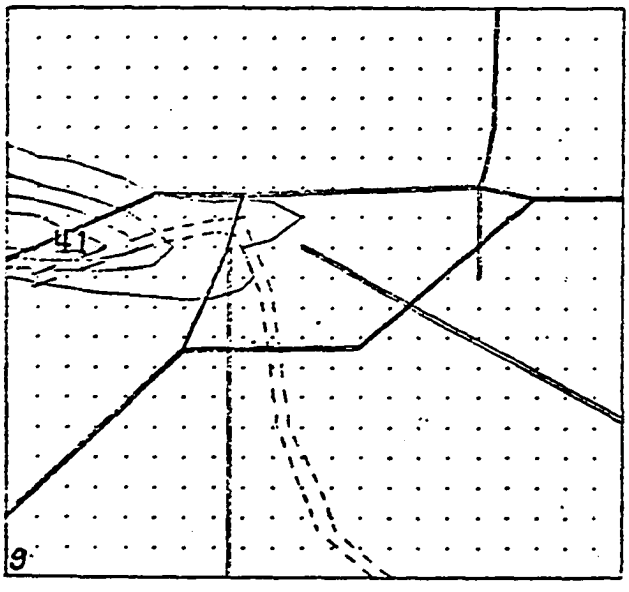

SO2 HRLY AVG 7 MAR 73 2100 CST
WIND 030/2.6 M/SEC CLOUD COVER .90
CONCENTRATION IN MICROGRAMS PER CUBIC METER
LOW CONTOUR VALUE=5.0 CONTOUR INTERVAL=10.0

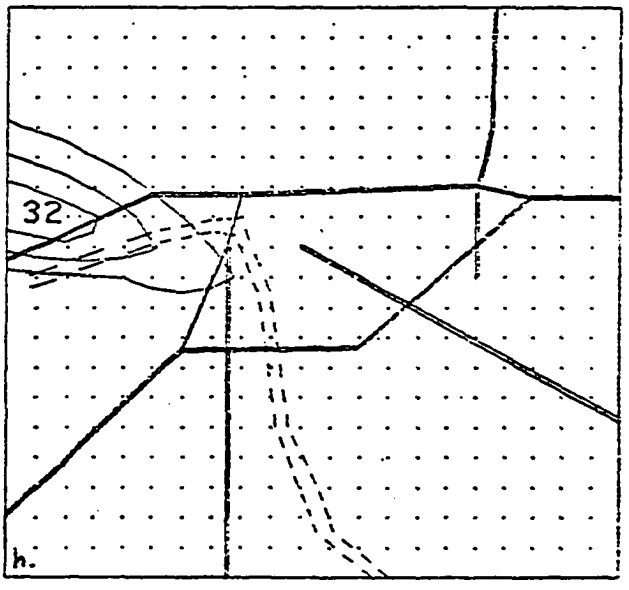

SO2 HRLY AVG 8 MAR 73 0000 CST
WIND 110/4.1 M/SEC CLOUD COVER .60
CONCENTRATION IN MICROGRAMS PER CUBIC METER
LOW CONTOUR VALUE=5.0 CONTOUR INTERVAL=10.0

Figure 21 (continued).

Mean daily concentrations for March 7, 1973 of CO and SO_2 are shown in Figures 22a and 22b. Since there was so much variation in dispersion patterns from hour to hour, the maximum predicted SO_2 twenty-four hour average concentration (14 micrograms/meter^3) is much less than the predicted maximum hourly concentrations (24-63 micrograms/meter^3).

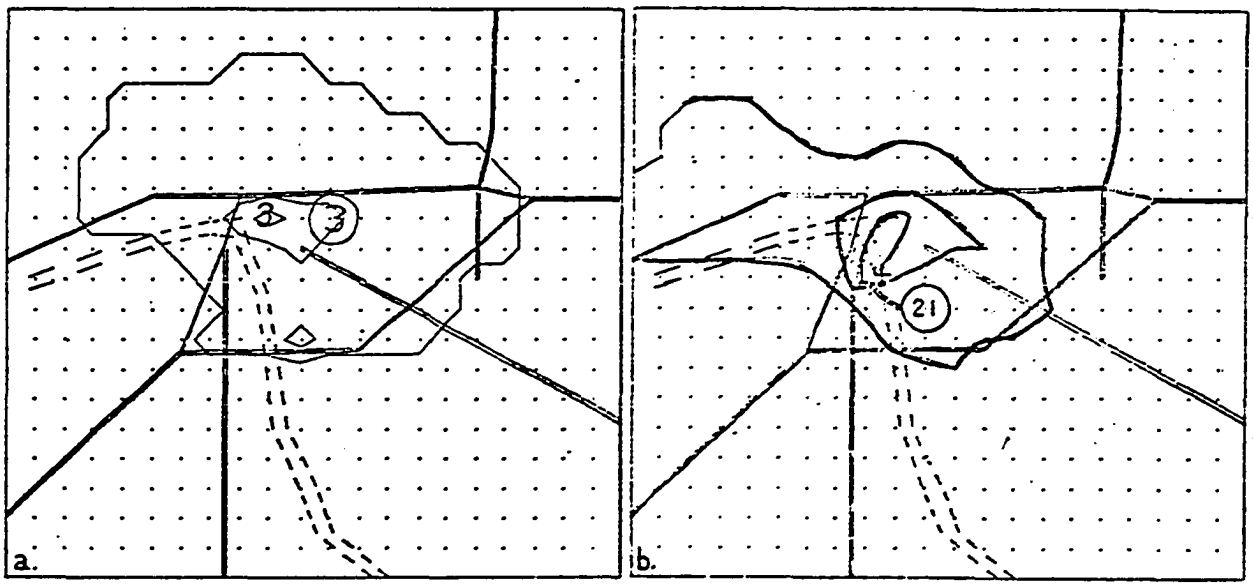

Figure 22: Average daily concentrations of carbon monoxide and sulfur dioxide.

CHAPTER V

EXTENSIONS AND MODIFICATIONS OF THE DIFFUSION WIND MODEL

The development of the diffusion wind atmospheric dispersion model is not limited to the level described in this dissertation, nor are the uses of the model confined to those shown.

The treatment of meteorological and emission parameters can always be made more involved, but the additional computation cost and effort should be weighed against the expected increase in accuracy or spatial and temporal resolution of prediction. This is particularly necessary when certain meteorological or emission variations are known to exist, but are not known or understood enough to estimate or specify from available data. The error in estimation of variations may actually cause the quality of the predictions of the model to decrease. Modeling of horizontal meteorological variations are examined in this light in section A.

Often in environmental assessments necessary for industrial construction or operation, a single point source is modeled. The only predictions may be for that single source, although regulatory agencies may examine existing

air quality in order to determine the maximum allowable pollution increment. Recommended modification of the diffusion wind model for examination of a single source are given in section B.

Scaling down of the diffusion wind model for prediction on the scale of a central business district or street intersection is analyzed in sections C and D, while increasing the scope of the model for synoptic scale dispersion prediction is analyzed in section E.

Finally, operational or regulatory use and planning use of the diffusion wind model are examined in section F and G. Emphasis is given in operational use to thorough calibration of the model.

A. Horizontal Meteorological Variation

In development of the diffusion wind model (Shannon, 1972), the wind and stability fields varied horizontally as well as vertically and temporally. The horizontal variation was due to modeling of mountainous terrain and the resulting effect upon meteorological parameters. The main difference in programming is that a number of computations which are made only once for each layer in the current version were made for each block in the 1972 work; this meant that many arrays which are currently one-dimensional were then three-dimensional. Modeling of horizontal variations of wind and stability would approximately double core storage requirements and would increase computation time by about fifty percent.

For the Tulsa urban area, horizontal variations of the wind field should be minor on a time scale of one hour or longer. The Arkansas River is too narrow to produce a significant variation in the one mile horizontal scale of the model, while terrain variations across the urban area are minor. In any case, no study of the horizontal variation of the Tulsa wind field is available.

Variations of mixing in the horizontal would be even harder to determine. The tall buildings in the central business district (CBD) increase gustiness and would increase mixing, but the CBD covers less than 1% of the total area modeled. For a large metropolis, the variation in the urban surface would be much more important.

B. Single Point Source

For examination of dispersion for a single point source, the dimensions of grid blocks in the diffusion wind model should be altered. The optimal number and depth of layers would depend upon the stack parameters, but in general there should be several layers between the mouth of the stack and the surface and there should be several layers above the stack, in order that significant changes in wind speeds could cause the plume to rise into different layers. Total model depth should be sufficient to contain the plume within the system, even in the case of light winds.

The choice of the horizontal grid increment is partly dependent upon the magnitude of the stack parameters.

In general, the higher the stack and plume rise, the larger the horizontal grid increment can be. Another important factor is the time and space scale of the question being examined. The question "Where is the thirty-minute maximum likely to occur and how high will it be?" calls for a finer resolution than the question "What pattern of daily average concentration is expected?". Another important factor is the number and location of sensors. Since there is only one prediction per grid block, it would be sub-optimal to have two or more sensors located inside the same block, as two observations would be compared to a single prediction.

C. Central Business District

When the central business district (CBD) is modeled, a necessary concept is differentiation between model blocks which are atmosphere and model blocks which are terrain (buildings). Due to the street "canyons", automobile emissions are actually being dispersed into a more confined volume than would be the case in the open countryside. In previous work (Shannon, 1972) which modeled the El Paso area, mountains were modeled by combinations of blocks. The terrain blocks were differentiated from atmosphere blocks by a 0-1 indicator array. Pollution was not allowed to diffuse into terrain blocks, but instead was redestributed to the atmospheric blocks. The same algorithm could be used for the CBD.

A more difficult problem is modeling of the wind field, which would be channelized by the buildings. Computation of a wind field through input of values for the upwind

edge of the grid and application of the equation of continuity for an incompressible fluid might lead to vertical wind components which were unreasonably large. The vertical wind field in the CBD would be much more significant than in the open countryside, but it might be more representative of the actual diffusion conditions to have very strong vertical diffusion in the canyons rather than strong vertical wind components.

It might prove to be more efficient as far as programming is concerned to have non-uniform horizontal blocks. The grid blocks representing buildings could be large squares, the grid blocks representing intersections could be small squares, and grid blocks representing streets might be oblong in one direction or the other.

D. Street Intersection

The key to accurate modeling of a street intersection would be proper representation of the traffic flow. Close cooperation with traffic authorities would be necessary in order to obtain adequate data. It would be necessary to model individual traffic lanes as sources. Since emissions are higher when cars are idling at a traffic light than when traffic is flowing through an intersection, queuing theory might be necessary in emission algorithms.

For modeling on the spatial scale of a single street intersection, grid block dimensions would be no more than 5-10 meters, and thus the time increment could be no greater than a few seconds. The time scale of question to be examined by the

model would likely be less than one hour.

Many of the techniques to be applied and difficulties to be overcome in CBD modeling, such as building block indicators and generation of a representative wind field, would also apply to a street intersection model.

E. Synoptic Scale Dispersion

There is no theoretical obstruction to adaptation of the diffusion wind model to advection and diffusion of air pollution in a synoptic (several state) scale. Dimensions would need to be increased considerably. Horizontal dimensions might be in the range 10-50 kilometers, while the total vertical depth should probably be at least 3000 meters. If winds and wind forecasts from a numerical model were available, it would be desirable to overlay as much as possible the diffusion wind grid and the numerical model grid.

Since grid dimensions would be large, the time step would also be large. It is likely that modeling might be extended for periods up to a week, since the interesting situation might be a large stagnant high. Necessary algorithms for synoptic scale dispersion include an efficient emission routine, since the smallest scale of interest might be an entire urban area, and a daily variation of the depth of the mixing layer. The magnitude of the diffusion wind components might be considerably different than the values used for the Tulsa urban area.

F. Operational Use

Operational use of the diffusion wind model, or any comparable dispersion model, requires accurate data. Currently, emission data are total or average values for the year. Major sources could be required or requested (depending upon governmental regulatory powers) to report occurring or predicted emission rates which are significantly different from average rates. Traffic counters could be automated and used to estimate traffic volume and resulting emissions relative to the normal or expected patterns.

A simple form of meteorological data input currently available would be hourly observations from the Tulsa weather station of wind, temperature, and cloud cover, along with the lower portion of the twice daily Oklahoma City soundings. The model could be run with current meteorological conditions, or it could be run with a forecast pattern.

It would be desirable to have meteorological data which were more detailed in space and time. Vertical data could be obtained from pibals or tethered balloons. If funds were available, an urban area such as Tulsa could be instrumented with 5-10 optimally located automated surface observation sites and 2-4 instrumented towers. Optimality of site location could be determined by using experimental design techniques of Yerg (1973), Kays (1974) or Brady (1975). A four-dimensional perturbation on the urban wind field could be generated by an urban heat island model such as that of

Wagner and Yu (1972). This perturbation plus noise could be added to a wind field in which the winds varied vertically as in an Ekman spiral (increasing and veering with height), and a non-linear programming search technique such as that applied by Brady could be used to select an optimal location of observation sites. Optimality would be determined by the best reproduction of input signal, or maximum reduction of observed variance, through use of the objective analysis (O.A.) technique of Eddy (1973). After sites had been selected and sensors installed, the observation data could be used to generate four-dimensional urban wind and stability fields, again using the Eddy O.A. technique; the wind field would then be an input to a version of the diffusion wind model which allowed horizontal variation of meteorological parameters.

Sites for air quality samplers could be optimally selected through similar techniques, with the input signal being generated by results from the diffusion wind model. If the samples were on-line, observations could pinpoint episode potential. Different strategies in short-term emission control could be evaluated quickly and the optimal strategy selected. The above scenario assumes either public-spirited industries or powerful regulatory agencies.

G. Planning Use

Planning use of the diffusion model would be on a different time scale than regulatory use. General trends would be of greater importance than specific cases. The

planning agencies would not be investigating time strategy of emissions, but rather whether the emissions should be allowed in that location at all.

A useful technique would be to investigate past data for occasions when air pollution readings were significantly high, and then to obtain accurate meteorological and emission data for that date.

To this the planning agency would add the effect of an additional source at different sites, in order to examine the total effect upon air quality. The effect of new traffic arteries or new urban development could be investigated in similar fashion.

CHAPTER VI

SUMMARY AND CONCLUSIONS

The diffusion wind atmospheric dispersion model has made representative predictions of pollution concentration fields under conditions of temporal and vertical variation of wind and stability and temporal variation of emission rates. The primary time scale for which the diffusion wind model is needed is a period of a few hours to a week in duration; during such a time span the temporal sequence of spatial variations has a critical effect upon dispersion results. This time scale is characteristic of air pollution episodes; the lower end of the time scale applies to short-term fumigation conditions while the upper end applies to large stagnant high pressure systems.

The diffusion wind model is a box model in representation of the atmosphere. The key diffusion mechanism of the model is the concept of the diffusion wind, which expands and diffuses plumes or clouds of pollution at the same time that the regular wind transports the pollution. Increasing the magnitudes of the components of the diffusion wind increases mixing and diffusion. An objective relationship between the magnitudes of the components and stability classes was

developed.

The diffusion wind model was applied to a 440 square mile area containing the city of Tulsa, Oklahoma. Real meteorological, emission, an air quality data were used, and variables and assumptions in the model were tested for their effect upon predictions.

Predicted sulfur dioxide concentrations resulting from elevated point sources were found in some cases to be twice as large when Holland's plume rise formula was used instead of Briggs' plume rise formula. The choice of surface deposition over surface reflection reduced surface concentrations about 10-20%. The most important factor in concentrations of pollutants emitted mainly by traffic was found to be the wind speed. Predicted sulfur dioxide concentrations were strongly affected by the wind speed, and were found to increase by about one third when the general wind direction was along the orientation of major Tulsa sources rather than perpendicular to the orientation. Traffic related pollutants showed the most diurnal and weekly variation in modeled results.

Comparison of observed and predicted concentrations was limited, because of a lack of adequate air quality measurements in space and time. In test cases the diffusion wind model showed greatest predictive accuracy for nitrogen dioxide (emitted largely by widespread traffic sources). Prediction of sulfur dioxide concentrations gave representative values, although the lack of upper air data may have

lead to a biasing of plume orientation. Predictions of particulate concentrations by the model were unsatisfactory, due mainly to an incomplete emission inventory.

The diffusion wind model can be increased or decreased in scale. Accuracy of predictions will be contingent upon accuracy in modeling the corresponding wind, stability, and emission fields. The model would be very useful in testing the effect of emission strategies because of the temporal and spatial variation capabilities of the model.

There is no final version of the diffusion wind atmospheric dispersion model. The model was developed to make fullest possible use of available data, while maintaining computational efficiency. The problems being examined and the information available will vary; so will the specifics of the model. The basic concept and mechanisms of the model will remain.

REFERENCES

Brady, P.J., 1975: "Optimal Sampling and Analysis Using Two Variables and Modelled Cross-Covariance Functions," Proc. 4th Conf. on Prob. and Stat. in the Atmos. Sciences, Tallahassee, FL.

Briggs, G.A., 1971: "Some Recent Analyses of Plume Rise Observations," Proc. of the Second International Clean Air Congress, New York, Academic Press.

Busse, A.D. and J.R. Zimmerman, 1973: User's Guide for the Climatological Dispersion Model, EPA-R4-73-024.

Crawford, K.C., A. Eddy, and W.J. Parton, Jr., 1971: "Customer-Tailored Forecasts Using Markov Chains and Decision Theory," Int. Symposium on Prob. and Stat. in the Atmos. Sciences, Honolulu, 100-105.

Crawford, K.C. and H.R. Hudson, 1970: Behavior of Winds in the Lowest 1500 Feet in Central Oklahoma: June 1966-May 1967, U.S. Dept. of Commerce, ERLTM-NSSL 48.

Eddy, A., 1973: "The Objective Analysis of Atmospheric Structure," J. Meteor. Soc. of Japan, vol. 51, 450-457.

Goff, R.C. and H.R. Hudson, 1972: The Thermal Structure of the Lowest Half Kilometer in Central Oklahoma: December 9, 1966 - May 31, 1967, U.S. Dept. of Commerce, ERL NSSL-58.

Halitsky, J. and K. Woodward, 1974: "Atmospheric Dispersion Experiments at a Nuclear Power Plant Site Under Light Wind Conditions," Proc. Symposium on Atmos. Diff. and Air Poll., Santa Barbara, CA., 172-175.

Holland, J.Z., 1953: "A Meteorological Survey of the Oak Ridge Area," AEC Report ORO-99, Washington, D.C., 554-559.

Kays, M.D., 1974: Optimal Sampling of a Stratospheric Sudden Warming, PhD dissertation, Dept. of Meteorology, University of Oklahoma.

Montgomery, T.L., W.B. Norris, F.W. Thomas, and S.B. Carpenter, 1973: "A Simplified Technique Used to Evaluate Atmospheric Dispersion of Emissions from Large Power Plants," J. Air Poll. Control Assoc., vol. 23, 388-394.

Schuck, E.A., A.P. Altshuller, D.S. Barth, and G.B. Morgan, 1970: "Relationship of Hydrocarbons to Oxidents in Ambient Atmospheres," J. Air Poll. Control Assoc., vol. 20, 297-302.

Shannon, J.D., 1972: A Diffusion Wind Atmospheric Model, Master's thesis, Dept. of Meteorology, University of Oklahoma.

Shannon, J.D., 1974: "Dispersion of Radioactive Particles by the Diffusion Wind Model," Report for White Sands Missile Range, Task Order 74-60.

Singer, I.A., and P.C. Freudenthal, 1972: "State of the Art of Air Pollution Meteorology," Bull. Amer. Meteor. Soc., vol. 53, 545-547.

Sklarew, R.C., A.J. Fabrick, and J.E. Prager, 1971: A Particle-in-Cell Method for Numerical Solution of the Atmospheric Diffusion Equation, and Application to Air Pollution Problems, Div. of Meteor., Nat. Environ. Research Cen., report 35R-844.

Turner, B.D., 1969: Workbook of Atmospheric Dispersion Estimates, Public Health Service Pub. No. 999-AP-26.

Wagner, N.K. and T. Yu, 1972: "Heat Island Formation: A Numerical Experiment," Conf. on Urban Environment, Philadelphia, 83-88.

Yerg, M., 1973: An Optimal Sampling and Analysis Methodology, PhD dissertation, Department of Meteorology, University of Oklahoma.

APPENDICES

A. Calculation of Diffusion Wind Components

In order to develop a formula for objective calculation of the magnitudes of the diffusion wind components, a number of simplifying assumptions are necessary. For calculation of the vertical diffusion wind component (AUSZ in the computer program), assume that the diffusion wind model consists of two layers, with total reflection from the top and bottom, a zero mean wind, and no horizontal diffusion. The upper layer is K times as thick as the lower layer (K can be less than 1) and the initial concentration gradient, ΔC_o, is due to a higher concentration in the lower layer. The sole dispersion process simulated will be vertical diffusion.

After n time steps or iterations, the vertical concentration gradient will be fraction Y of the original gradient ΔC_o. Y will be a relatively large fraction for stable cases and will approach zero as stability decreases. What value of AUSZ corresponds to a particular value of Y?

In the derivation which follows, ΔT is the time step, ΔZ is the thickness of the bottom layer, and $Z = (AUSZ*\Delta T)/\Delta Z$. Assume that the volume of the lower block

is one (unit unspecified). In order to simplify computations, after each time step the lower value of the two concentrations will be converted to the appropriate mass for each layer and will be removed from further calculations.

Iteration	Lower layer mass (Lower concentration)	Upper layer mass (Upper concentration*K)	Gradient of concentration
0	M	0	$\Delta C_o = M$
1	$(1-\frac{Z}{1+Z})M$	$(\frac{Z}{1+Z})M$	$(1-\frac{Z}{1+Z}-\frac{Z}{K(1+Z)})M$
2	$(1-\frac{Z}{1+Z})(1-\frac{Z}{1+Z}-\frac{Z}{K(1+Z)})M$	$\frac{Z}{1+Z}(1-\frac{Z}{1+Z}-\frac{Z}{K(1+Z)})M$	$(1-\frac{Z}{1+Z}-\frac{Z}{K(1+Z)})^2M$
3	$(1-\frac{Z}{1+Z})(1-\frac{Z}{1+Z}-\frac{Z}{K(1+Z)})^2M$	$\frac{Z}{1+Z}(1-\frac{Z}{1+Z}-\frac{Z}{K(1+Z)})^2M$	$(1-\frac{Z}{1+Z}-\frac{Z}{K(1+Z)})^3M$
.	.	.	.
.	.	.	.
.	.	.	.
n	$(1-\frac{Z}{1+Z})(1-\frac{Z}{1+Z}-\frac{Z}{K(1+Z)})^{n-1}M$	$\frac{Z}{1+Z}(1-\frac{Z}{1+Z}-\frac{Z}{K(1+Z)})^{n-1}M$	$(1-\frac{Z}{1+Z}-\frac{Z}{K(1+Z)})^nM$

$$(1-\frac{Z}{1+Z}-\frac{Z}{K(1+Z)})^n = Y$$

$$Z = \frac{K(1-Y^{1/n})}{KY^{1/n}+1}$$

$$AUSZ = \frac{\Delta Z \cdot K(1-Y^{1/n})}{\Delta T(KY^{1/n}+1)} \qquad (A1)$$

A similar formula for the horizontal diffusion wind component AUS can be derived if simplifying assumptions analogous to those for the vertical case are made. Assume that the diffusion wind model consists of two blocks of identical dimensions in one layer, with reflection from the top, bottom, and outer sides, and a zero mean wind. The

only dispersion process simulated will be horizontal diffusion between the two blocks. It can be shown that

$$AUS = \frac{\Delta X(1-W^{1/n})}{\Delta T(W^{1/n}+1)} \qquad (A2)$$

where ΔX is the horizontal grid length and W is the fraction of the original concentration remaining after n time steps.

The most widely used dispersion model is the Gaussian model of Pasquill and Gifford, as described by Turner (1969). A method was devised to relate sets of values for Y and W to each Pasquill-Gifford stability class.

Block-average Gaussian plumes were compared to diffusion wind model plumes for each stability class. The plume came from a single source in the middle layer of a version of the diffusion wind model similar to that used to model the Tulsa airshed.

For both models the plumes were allowed to deposit pollutant onto the surface and diffuse above the 310 meter top of the modeled atmosphere. For the unstable cases, particularly for the Gaussian model, the plumes several miles downwind of the source were predicted to have undergone so much vertical diffusion that resulting concentrations inside the 310 meter depth were very low. In a real situation there would probably be a cap or inversion over the mixing layer which would limit the plume dilution. For other than the very unstable cases, minor adjustments in the

first-guess values of Y and W led to diffusion wind plumes which were similar to the corresponding Gaussian plumes.

The values for Y and W which were found by this plume comparison method after one hour of dispersion are shown in Table 5.

TABLE 5.--Diffusion Parameters Calculated for the Diffusion Wind Atmospheric Dispersion Model.

	Stability Class					
	A	B	C	D	E	F
Y	.0001	.0005	.001	.01	.05	.20
W	.05	.10	.25	.50	.75	.85

It should be noted that the values for Y and W apply to the Tulsa version of the diffusion wind model, and would require adjustment if the diffusion wind model were changed considerably.

Tables 6a and 7a show horizontal and vertical slices along a Gaussian plume for neutral stability (P-G class D), while Tables 6b and 7b show horizontal and vertical slices along the plume from the diffusion wind model under the same conditions. It can be seen that the two plumes compare quite closely.

Examples of the values computed for AUS (horizontal diffusion wind), AUSZU (vertical diffusion wind upward from a block), and AUSZL (vertical diffusion wind

TABLE 6.--Comparison of Horizontal Slices Along a Neutral Stability Plume for the Gaussian Model (a) and the Diffusion Wind Model (b).

a. GAUSSIAN PLUME HORIZONTAL SLICE

0.0	0.0	0.0	0.0	0.0	0.0	0.0	0.0	0.0	0.0	0.0	0.0	0.0
0.0	0.0	0.0	0.0	0.0	0.0	0.0	0.0	0.0	0.0	0.00	0.00	0.00
0.0	0.0	0.0	0.0	0.0	0.0	0.0	0.00	0.00	0.00	0.00	0.00	0.00
0.0	0.0	0.0	0.0	0.00	0.00	0.00	0.00	0.00	0.01	0.01	0.02	0.03
0.0	0.00	0.02	0.09	0.20	0.32	0.41	0.48	0.53	0.57	0.60	0.61	0.62
14.22	9.12	7.19	5.80	4.74	4.05	3.44	2.95	2.56	2.28	2.03	1.82	1.64
0.0	0.00	0.02	0.09	0.20	0.32	0.41	0.48	0.53	0.57	0.60	0.61	0.62
0.0	0.0	0.0	0.0	0.00	0.00	0.00	0.00	0.00	0.01	0.01	0.02	0.03
0.0	0.0	0.0	0.0	0.0	0.0	0.0	0.00	0.00	0.00	0.00	0.00	0.00
0.0	0.0	0.0	0.0	0.0	0.0	0.0	0.0	0.0	0.0	0.00	0.00	0.00
0.0	0.0	0.0	0.0	0.0	0.0	0.0	0.0	0.0	0.0	0.0	0.0	0.0

b. DIFFUSION WIND PLUME HORIZONTAL SLICE

0.0	0.0	0.0	0.0	0.0	0.0	0.0	0.0	0.0	0.0	0.0	0.0	0.0
0.0	0.0	0.0	0.0	0.0	0.0	0.0	0.00	0.00	0.00	0.00	0.00	0.01
0.0	0.00	0.02	0.04	0.06	0.07	0.09	0.10	0.02	0.06	0.09	0.01	0.01
0.05	0.05	0.04	0.14	0.17	0.18	0.05	0.22	0.38	0.07	0.49	0.09	0.13
0.98	1.23	1.37	1.43	1.43	1.40	1.36	1.34	1.29	1.21	1.18	1.09	1.03
23.12	15.93	11.82	9.25	7.49	6.22	5.27	4.51	3.91	3.41	2.99	2.63	2.33
0.99	1.23	1.37	1.43	1.42	1.40	1.36	1.34	1.29	1.21	1.18	1.09	1.03
0.05	0.05	0.04	0.14	0.17	0.18	0.05	0.22	0.38	0.07	0.49	0.09	0.13
0.0	0.00	0.02	0.04	0.06	0.07	0.09	0.10	0.02	0.06	0.09	0.01	0.01
0.0	0.0	0.0	0.0	0.0	0.0	0.0	0.00	0.00	0.00	0.00	0.00	0.01
0.0	0.0	0.0	0.0	0.0	0.0	0.0	0.0	0.0	0.0	0.0	0.0	0.0

TABLE 7.--Comparison of Vertical Slices Along a Neutral Stability Plume for the Gaussian Model (a) and the Diffusion Wind Model (b).

a. GAUSSIAN PLUME VERTICAL SLICE

0.08	0.65	1.14	1.50	1.67	1.68	1.64	1.56	1.47	1.38	1.30	1.21	1.13
5.99	6.12	5.55	4.84	4.14	3.62	3.13	2.73	2.40	2.14	1.92	1.73	1.57
14.22	9.12	7.19	5.80	4.74	4.05	3.44	2.95	2.56	2.28	2.03	1.82	1.64
11.39	8.34	6.80	5.58	4.61	3.96	3.37	2.90	2.53	2.25	2.01	1.80	1.63
8.31	7.38	6.30	5.30	4.43	3.83	3.29	2.84	2.48	2.21	1.98	1.78	1.61

b. DIFFUSION WIND PLUME VERTICAL SLICE

0.12	0.50	0.89	1.15	1.22	1.23	1.18	1.10	1.01	0.92	0.83	0.74	0.67
4.42	5.28	5.12	4.68	4.14	3.65	3.22	2.83	2.50	2.21	1.96	1.73	1.54
23.12	15.93	11.82	9.25	7.49	6.22	5.27	4.51	3.91	3.41	2.99	2.63	2.33
7.48	8.93	8.68	7.89	7.01	6.17	5.44	4.78	4.22	3.73	3.31	2.93	2.61
0.12	1.45	2.60	3.25	3.50	3.51	3.36	3.14	2.88	2.62	2.37	2.13	1.91

downward from a block) are shown in Table 8. For purposes of claculation of AUSZL in the bottom layer and AUSZU in the top layer, a K value of 2 is used.

TABLE 8.--Examples of Calculated Diffusion Wind Component Values (meters/second).

WIND SPEED 2.0 METERS/SECOND TIME INCREMENT 720.0 SECONDS

HORIZONTAL GRID INCREMENT 1609. METERS							VERTICAL GRID INCREMENTS											
				AUS						AUSZU						AUSZL		
LAYER	1	2	3	4	5	6	1	2	3	4	5	6	1	2	3	4	5	6
P-G STAB. CLASS																		
A	.650	.650	.650	.650	.650	.650	.0089	.0177	.0355	.0710	.1420	.2840	.0089	.0054	.0108	.0217	.0433	.0866
B	.506	.506	.506	.506	.506	.506	.0075	.0151	.0302	.0604	.1208	.2416	.0075	.0049	.0098	.0196	.0391	.0781
C	.308	.308	.308	.308	.308	.308	.0069	.0138	.0277	.0554	.1108	.2215	.0069	.0046	.0092	.0185	.0370	.0739
D	.155	.155	.155	.155	.155	.155	.0047	.0093	.0186	.0372	.0745	.1489	.0047	.0035	.0070	.0139	.0279	.0558
E	.064	.064	.064	.064	.064	.064	.0030	.0060	.0119	.0239	.0477	.0955	.0030	.0025	.0045	.0089	.0196	.0393
F	.036	.036	.036	.036	.036	.036	.0016	.0031	.0062	.0125	.0250	.0499	.0016	.0014	.0028	.0056	.0112	.0224

WIND SPEED 5.0 METERS/SECOND TIME INCREMENT 300.0 SECONDS

HORIZONTAL GRID INCREMENT 1609. METERS							VERTICAL GRID INCREMENTS											
				AUS						AUSZU						AUSZL		
LAYER	1	2	3	4	5	6	1	2	3	4	5	6	1	2	3	4	5	6
P-G STAB. CLASS																		
A	.666	.666	.666	.666	.666	.666	.0053	.0185	.0371	.0741	.1482	.2964	.0053	.0072	.0145	.0290	.0580	.1160
B	.513	.513	.513	.513	.513	.513	.0076	.0152	.0303	.0607	.1214	.2428	.0076	.0062	.0124	.0247	.0494	.0989
C	.309	.309	.309	.309	.309	.309	.0069	.0137	.0275	.0549	.1099	.2197	.0069	.0057	.0114	.0228	.0455	.0911
D	.155	.155	.155	.155	.155	.155	.0045	.0090	.0180	.0360	.0719	.1439	.0045	.0040	.0079	.0158	.0317	.0634
E	.064	.064	.064	.064	.064	.064	.0029	.0058	.0115	.0230	.0461	.0921	.0029	.0026	.0053	.0106	.0212	.0424
F	.036	.036	.036	.036	.036	.036	.0015	.0030	.0061	.0122	.0244	.0487	.0015	.0015	.0029	.0058	.0116	.0233

WIND SPEED 9.0 METERS/SECOND TIME INCREMENT 200.0 SECONDS

HORIZONTAL GRID INCREMENT 1609. METERS							VERTICAL GRID INCREMENTS											
				AUS						AUSZU						AUSZL		
LAYER	1	2	3	4	5	6	1	2	3	4	5	6	1	2	3	4	5	6
P-G STAB. CLASS																		
A	.668	.668	.668	.668	.668	.668	.0051	.0182	.0364	.0729	.1457	.2914	.0051	.0077	.0154	.0308	.0616	.1233
B	.514	.514	.514	.514	.514	.514	.0075	.0149	.0298	.0596	.1192	.2385	.0075	.0065	.0130	.0259	.0519	.1038
C	.310	.310	.310	.310	.310	.310	.0067	.0135	.0270	.0540	.1079	.2158	.0067	.0059	.0119	.0238	.0475	.0951
D	.155	.155	.155	.155	.155	.155	.0044	.0089	.0177	.0354	.0709	.1417	.0044	.0041	.0081	.0163	.0325	.0651
E	.064	.064	.064	.064	.064	.064	.0028	.0057	.0114	.0228	.0455	.0911	.0028	.0027	.0054	.0108	.0215	.0431
F	.036	.036	.036	.036	.036	.036	.0015	.0030	.0060	.0121	.0242	.0484	.0015	.0015	.0029	.0059	.0117	.0235

The vertical gradient of temperature, $\frac{\Delta T}{\Delta Z}$, and the average wind direction range, R_θ, associated with the Pasquill-Gifford stability classes, are shown in Table 9 (Halitsky and Woodward, 1974).

TABLE 9.--Vertical Temperature Gradient and the Wind Direction Ranges Associated with Pasquill-Gifford Stability Class.

Pasquill Stability Class	Average Vertical Temp. Gradient $\Delta T/\Delta z$ (deg C/100 m)	Average Wind Direction Range, R_θ (deg)
A	$\Delta T/\Delta z \leq -1.9$	≥ 136
B	$-1.9 < \Delta T/\Delta z \leq -1.7$	106-135
C	$-1.7 < \Delta T/\Delta z \leq -1.5$	76-105
D	$-1.5 < \Delta T/\Delta z \leq -0.5$	46-75
E	$-0.5 < \Delta T/\Delta z \leq +1.5$	23-45
F	$+1.5 < \Delta T/\Delta z$	≤ 22

B. Computation of Pollutant Emissions from Traffic

The traffic count data available for Tulsa included average daily traffic counts for the freeways and major streets, maximum hourly counts for the central business district, and average daily trip counts by square mile for internal traffic.

For freeways and major streets, it was necessary to have traffic counts every mile. If no observed data were available, interpolation between the nearest counts provided estimated counts. An average vehicle speed of 50 mph was assumed for freeways and a speed of 25 mph was assumed for city streets. Emission rates are shown in Table 10. The total emissions per square mile were calculated by including any counts within the section, and the values converted to tons per year for each pollutant.

Since CBD counts were collected in a much denser network, it was assumed that each car was counted ten times per mile. An average CBD traffic speed of 15 mph was assumed. The counts were totaled in each section containing part of the CBD, with the average daily count considered to be 20.4 times the maximum hour count, .1 vehicle mile assumed for each count, and emission rates as shown in Table 10. Total emissions were calculated in tons per year.

TABLE 10.--Emission Rates in Grams Per Vehicle-Mile.

	Freeways (50 mph)	Major Streets (25 mph)	Interior Traffic (25 mph)	CBD (15 mph)
CO	30	50	50	79
HC	5.5	7.6	7.6	10
NO_2	7.2	5.7	5.7	5
Particulates	.58	.58	.58	.58
SO_2	.20	.20	.20	.20

Each interior traffic round trip was assumed to be .6 mile, with an average vehicle speed of 25 mph. Emission rates assume are shown in Table 10. Results were expressed in tons per year per square mile.

In the diffusion wind model, all traffic sources are lumped together before being given a daily and hourly variation. Accuracy of emission data would be improved if each type of traffic source were given typical temporal variations from observed data.

C. Climate Generator

If dispersion simulations which do not correspond to a specific time and the observed values associated with that time are to be made, a climate generator can be used as the source of meteorological parameter values. An advantage of using a climate generator instead of inserting subjectively determined values is that the modeler does not bias the values. It is important that the climate generator provides values statistically consistent with a sequence of observed values, in order to make air quality productions resulting from use of the climate generator typical of actual air quality.

The climate generator which was developed for use with the diffusion wind model produces a daily resultant wind speed and direction, a daily arithmetic mean wind speed, and a percentage of possible daily sunshine received.

The daily resultant wind (after being given hourly and vertical variations by HMET) is used to advect the pollutants. The purpose of examining the arithmetic mean speed is to minimize underestimation of dispersion on days when there is a wind shift or wide variation in wind direction. An Oklahoma day with a frontal passage might have a resultant wind speed which was quite low, although pedestrians had to lean forward.

The stability parameter used (percentage of possible sunshine) is based solely upon daytime data.

However, cloudy days are more likely to be followed by cloudy nights than are clear days. Clear skies imply strong radiative flux and, when coupled with light wind speeds, can result in very stable nights and very unstable days.

The meteorological data used in construction of the climate generator were two years (1972-1973) of daily observations for Tulsa, including resultant daily wind speed and direction, average daily wind speed, and percentage of possible sunshine.

The first step was calculation of a twenty-four hour transition matrix, described by Crawford, Eddy and Parton (1971), for daily resultant wind direction. The daily observations were examined in sequence, with direction grouped into twelve categories of thirty degrees' width. As occurrences of a particular resultant wind direction category were encountered, the frequencies of occurrence the succeeding day of each of the twelve direction categories were accumulated; when the frequencies were normalized, a conditional probability vector whose components totaled 1.00 was created. A complete transition matrix is 12 x 12, and a daily resultant wind direction twenty-four hour transition matrix was calculated for each season. Seasonal resultant wind direction climatological probability vectors were also calculated.

Conditional probability matrices of the resultant wind speed (in categories one meter per second wide), as a function of the resultant wind direction category, were calculated for each season. Percentage of possible sunshine conditional probability matrices (in categories 10 percent wide) were similarly calculated by season as a function of resultant wind direction category. Conditional probability matrices for the excess of average wind speed over speed of the resultant wind (in categories .5 meter per second wide), as a function of the resultant wind speed, were calculated for each season. This increase, if large, is an indicator of significant wind shift or directional variation, and implies that dispersion should be greater than is implied by the resultant wind.

The transition matrices and conditional probability matrices were altered to cumulative form in order to facilitate computer searching. Random numbers from a rectangular distribution ranging from zero to one are compared to the elements in the proper row of the matrices. Since the values in the row now increase monotonically, the first value which exceeds the random number denotes the proper category. An initial wind direction category is generated from a climatological cumulative probability vector via this process. Based upon this initial resultant wind category, a resultant wind speed class and a percentage of possible sunshine are selected from their respective

cumulative probability matrices using other random numbers and a similar search technique. The increase of average wind speed over the speed of the resultant wind is selected in a similar manner, by use of the class of the resultant wind speed. The next day's resultant wind direction class is now generated by the random number search from the proper seasonal transition matrix and the result stored. The daily meteorological values are given random variations within their classes before use in the hourly meteorology generator (HMET). Examples of a cumulative transition matrix and a cumulative probability matrix are shown in Table 11 and Table 12.

TABLE 11.--Resultant Daily Wind Direction Cumulative 24-hour Transition Matrix from 1972-1973 Tulsa Observations.

season 1	degrees											
	015-045	045-075	075-105	105-135	135-165	165-195	195-225	225-255	255-285	285-315	315-345	345-015
15 - 45	0.1500	0.2000	0.2000	0.2500	0.3000	0.5000	0.6500	0.7000	0.7000	0.7000	0.7000	1.0000
45 - 75	0.0	0.1429	0.4286	0.4286	0.4286	0.7143	0.7143	0.8571	0.8571	0.8571	0.8571	1.0000
75 - 105	0.0	0.0	0.2500	0.2500	0.2500	0.5000	0.5000	0.5000	0.5000	0.5000	0.7500	1.0000
105 - 135	0.2000	0.2000	0.2000	0.2000	0.2000	0.4000	0.4000	0.4000	0.8000	0.8000	0.8000	1.0000
135 - 165	0.0769	0.0769	0.0769	0.1538	0.1538	0.4615	0.5385	0.5385	0.7692	0.8462	0.8462	1.0000
165 - 195	0.0500	0.0750	0.0750	0.0750	0.2250	0.5000	0.6500	0.7250	0.7250	0.7250	0.8750	1.0000
195 - 225	0.1250	0.2083	0.2083	0.2500	0.3333	0.6250	0.7917	0.7917	0.8333	0.8750	0.9167	1.0000
225 - 255	0.0	0.0	0.0	0.0	0.0	0.3333	0.5000	0.6667	0.8333	0.8333	1.0000	1.0000
255 - 285	0.2222	0.2222	0.2222	0.2222	0.3333	0.5556	0.5556	0.5556	0.5556	0.5556	0.7778	1.0000
285 - 315	0.0	0.0	0.0	0.0	0.0	0.0	0.0	0.0	0.0	0.0	0.3333	1.0000
315 - 345	0.0	0.0769	0.1538	0.1538	0.3077	0.3077	0.6154	0.6154	0.6923	0.6923	0.7692	1.0000
345 - 15	0.2162	0.2432	0.2432	0.2973	0.3243	0.4595	0.5946	0.6216	0.6486	0.6486	0.6757	1.0000

TABLE 12.--Resultant Daily Wind Speed Cumulative Probability Matrix 1972-1973 Tulsa Observations.

season 1	meters per second									
	0.0-1.0	1.0-2.0	2.0-3.0	3.0-4.0	4.0-5.0	5.0-6.0	6.0-7.0	7.0-8.0	8.0-9.0	9.0-UP
15 - 45	0.0500	0.1500	0.3000	0.6500	0.7000	1.0000	1.0000	1.0000	1.0000	1.0000
45 - 75	0.0	0.4286	0.4286	0.5714	1.0000	1.0000	1.0000	1.0000	1.0000	1.0000
75 - 105	0.2500	0.7500	1.0000	1.0000	1.0000	1.0000	1.0000	1.0000	1.0000	1.0000
105 - 135	0.0	0.6000	0.6000	1.0000	1.0000	1.0000	1.0000	1.0000	1.0000	1.0000
135 - 165	0.0	0.2308	0.3846	0.5385	0.7692	0.8462	0.9231	1.0000	1.0000	1.0000
165 - 195	0.0500	0.0750	0.2500	0.3750	0.4500	0.6000	0.7500	0.9250	1.0000	1.0000
195 - 225	0.1250	0.3750	0.5000	0.6667	0.7500	0.7917	0.8333	0.8750	0.9583	1.0000
225 - 255	0.0	0.2857	0.5714	0.8571	0.8571	1.0000	1.0000	1.0000	1.0000	1.0000
255 - 285	0.2222	0.3333	0.6667	0.8889	0.8889	0.8889	1.0000	1.0000	1.0000	1.0000
285 - 315	0.5000	0.5000	0.5000	1.0000	1.0000	1.0000	1.0000	1.0000	1.0000	1.0000
315 - 345	0.1429	0.2143	0.4286	0.5714	0.7143	0.8571	1.0000	1.0000	1.0000	1.0000
345 - 15	0.0270	0.1622	0.3514	0.5135	0.7027	0.8378	0.9459	1.0000	1.0000	1.0000